Accepted Manuscript

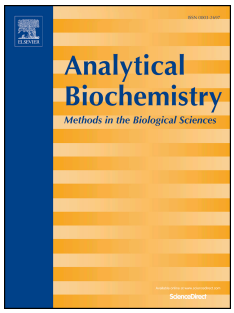

Designing binding kinetic assay on the bio-layer interferometry (BLI) biosensor to characterize antibody-antigen interactions

Vishal Kamat, Ashique Rafique

PII: S0003-2697(17)30334-2

DOI: 10.1016/j.ab.2017.08.002

Reference: YABIO 12762

To appear in: *Analytical Biochemistry*

Received Date: 15 February 2017

Revised Date: 3 August 2017

Accepted Date: 7 August 2017

Please cite this article as: V. Kamat, A. Rafique, Designing binding kinetic assay on the bio-layer interferometry (BLI) biosensor to characterize antibody-antigen interactions, *Analytical Biochemistry* (2017), doi: 10.1016/j.ab.2017.08.002.

Title: Designing Binding Kinetic Assay on the Bio-Layer Interferometry (BLI) Biosensor to Characterize Antibody-Antigen Interactions

Authors: Vishal Kamat *, Ashique Rafique
Biomolecular HTS Center, Therapeutic Proteins, Regeneron Pharmaceuticals
777 Old Saw Mill River Road, Tarrytown, NY, USA 10591

***Corresponding author**: Vishal Kamat,
Phone: +1-914-847-7771
Fax: +1-914-847-7453
Email: vishal.kamat@regeneron.com

Subject Category: Physical techniques

Highlights:

- High density antibody capture surface exhibited analyte rebinding and mass transport limitation (MTL)
- Kinetic assays performed on 0.1nm density antibody surface significantly reduced MTL and enabled characterization of picomolar affinity interactions.
- A total of 165 fully human antibodies binding to 14 different antigens with molecular weight ranging from 14kD to 105kD were characterized on Octet HTX, Biacore 4000 and MASS-1 and the results revealed that measured binding kinetic values were comparable across different biosensors.

Keywords: Biacore, Octet, Surface plasmon resonance, high throughput, antibody-antigen interaction, binding kinetics, affinity, monoclonal antibody

Abbreviations: surface plasmon resonance (SPR), surface plasmon resonance imaging (SPRi), bio-layer interferometry (BLI), monoclonal antibody (mAb), mass transport limitation (MTL), titration kinetic (TK), single cycle kinetic (SCK), conditioned media (CM), real-time label-free (RT-LF), association rate (k_a), dissociation rate (k_d), equilibrium dissociation constant (K_D), anti-human Fc (AHC), high capacity amine (HCA), Chinese Hamster Ovary (CHO)

ABSTRACT

The Octet biosensors provide a high-throughput alternative to the well-established surface plasmon resonance (SPR) and SPR imaging (SPRi) biosensors to characterize antibody-antigen interactions. However, the utility of the Octet biosensors for the accurate and reproducible measurement of binding rate constants of monoclonal antibodies (mAbs) is limited due to challenges such as analyte rebinding, and mass transport limitation (MTL). This study focuses on addressing these challenges and provides experimental conditions to reliably measure kinetics of mAb-antigen interactions. The mAb capture density of less than 0.6nm was found to be optimal to measure a wide range of binding affinities on Octet HTX. The titration kinetic and single cycle kinetic assays performed on Octet HTX generated reproducible binding kinetic parameters and correlated with the values measured on Biacore 4000 and MASS-1. Kinetic assays performed on 0.1nm density mAb surfaces significantly reduced MTL and enabled characterization of picomolar affinity mAbs. Finally, kinetic analysis performed on 150 antibodies to 10 antigens with molecular weights ranging from 21kD to 105kD showed concordance between Octet HTX, Biacore 4000 and MASS-1 ($R^2 > 0.90$). The data presented in this study suggest that under optimal experimental conditions, Octet biosensor is capable of generating kinetic values comparable to SPR/SPRi biosensors.

1. INTRODUCTION

The real-time, label-free (RT-LF) biosensors have become important biophysical tools in today's biopharmaceutical industry and are currently implemented in different stages of drug discovery and development. The kinetics of a drug molecule binding to its target is one of the vital parameters considered during the selection of a lead therapeutic agent. The RT-LF platforms enable quick measurement of association rate (k_a), dissociation rate (k_d) and equilibrium dissociation constant (K_D) of antibody-antigen interactions without the use of labeled reagents. During the primary screening of large libraries of unpurified monoclonal antibodies (mAbs) expressed in crude conditioned media (CM), kinetic screening performed using different RT-LF platforms enables rapid identification of a small panel of potential therapeutic candidates. Currently available high-throughput surface plasmon resonance (SPR) biosensors like Biacore 8k, and Biacore 4000 (formerly Biacore A100) (1,2) and surface plasmon resonance imaging (SPRi) based biosensors such as MASS-1, MASS-2, ProteOn XPR36, and IBIS MX96 (3-6) were designed to support the current throughput needs of biopharmaceutical industry. However, rapid screening of more than 2000 mAb clones from crude CM continues to be a challenge. This trade-off in the throughput of SPR/SPRi based biosensors is becoming a critical bottleneck in the discovery and development of drug molecules and is often cited as a key factor preventing their widespread application in biotherapeutic screening (7). Currently, there is an increasing demand for the availability of high throughput RT-LF platforms to accelerate drug screening and discovery.

In comparison to the SPR/SPRi biosensors, the bio-layer interferometry (BLI) based Octet biosensor is a relatively new RT-LF platform, but has the potential to support the current high throughput demands of the biopharmaceutical industry (8,9). The Octet biosensors differ from the SPR/SPRi based platforms in their detection system, sample delivery, sensitivity and throughput capability. The Octet biosensor is a plate based dip-and-read platform which measures interference patterns caused by the binding of protein dispensed in the sample plate to its binding partner, which is immobilized on the biosensor surface. Different Octet platforms are currently available with varying throughput ability. For example, the Octet HTX biosensor can simultaneously detect up to 96 interactions and is capable of screening 2000 mAb clones in approximately 3-4 hours; which would require approximately 3-4 days using the currently available high throughput SPR/SPRi biosensor. The measurement of binding events on Octet is minimally affected by the mismatch in the buffer conditions and hence the Octet biosensors were initially used to measure mAb titers in crude CM (10,11). Since then, diverse Octet applications have been established in different stages of mAb discovery and development workflow such as, kinetic analysis of mAb-antigen

interactions, epitope binning of mAbs, isotyping of mAb, cell line development, immunogenicity, pre-clinical assay development, and bioprocess development (8,12-18). Although Octet has accelerated the determination of binding affinities along with the off-rate ranking of mAbs expressed in crude CM (8,17), its application for kinetic analysis of mAbs has been limited due to the continued concerns on the reliability of measured binding rate constants (19,20). Moreover, lack of supporting evidence illustrating the reliability and reproducibility of the k_a, k_d, and K_D values measured on the Octet biosensors has further hindered its extended application for kinetic analysis of mAbs.

An abundance of currently available published literature provides guidelines on designing kinetics assays on SPR and SPRi biosensors, and diverse factors affecting the measurement of binding rate constants are mostly established (5,6,21-23). However, such aspects are not yet well understood for the Octet biosensors and literature providing appropriate experimental conditions for the measurement of binding rate constants is currently limited (8,12,19,24,25). Therefore, in this study we have investigated various factors that can potentially affect the characterization of antibody-antigen interactions. We have also validated the utility of the Octet biosensors to perform single cycle kinetic (SCK) assays by comparing the measured binding rate constants with those generated using the traditional titration kinetic (TK) assays on Octet HTX, Biacore 4000 and MASS-1 biosensors. In order to provide a higher confidence in the ability of Octet HTX to measure reliable and reproducible binding rate constants of mAb-antigen interactions, a total of 150 unique human mAbs binding to antigen with molecular weight ranging from 21kD to 105kD were later characterized in this study and the binding kinetic parameters measured on the Octet HTX were compared to those generated using the Biacore 4000 and MASS-1 biosensors. Our data demonstrate that under optimized experimental conditions, k_a, k_d and K_D values measured on the Octet HTX can correlate with the values generated using Biacore 4000 and MASS-1.

2. MATERIALS & METHODS:

2.1. Reagents

N-(3-dimethylaminopropyl)-N-ethylcarbodiimide (EDC) and N-hydroxysuccinimide (NHS), ethanolamine–HCl (Catalog# BR100633), anti-human Fc specific capture mAb (Catalog# BR-1008-39) and CM5 sensor chip (Catalog# BR-1005-30) were purchased from GE Healthcare. The high capacity amine (HCA) sensor chip (Catalog# SPR-AS-HCA) was purchased from Sierra Sensors GmbH while sodium acetate, pH 5.0 was purchased from Ricca Chemical (Catalog# 61-1). All recombinant proteins were expressed using stable Chinese Hamster Ovary (CHO) cell lines and purified in-house. The mAbs used in this study were fully human mAbs expressed with either human IgG1 or IgG4. The antigens used in the study are monomeric ecto-domains of the single transmembrane receptor expressed with a C-terminal myc-myc-6xHis tag. The antigens and mAbs expressed in CM were purified using the HisTalon superflow cartridge (Clontech) and the Protein A Fast Flow HiTrap cartridge (GE Healthcare) respectively, as reported previously (26).

2.2. Binding studies performed on Octet HTX

Before designing kinetic assays on Octet HTX, we investigated various factors such as buffer condition, orbital shake speed, and well plate that can assist in the generation of reliable kinetic data. We observed that binding assays performed in buffer containing 1 mg/mL BSA with orbital shake speed of 1000 rpm generated the best quality binding curves with minimal sensor to sensor variability and baseline drift. We also observed that binding studies performed using 384-tilted well plates generated minimal bulk shifts when the Octet biosensors were dipped in different wells. Therefore, all kinetic assays on Octet HTX were performed in freshly prepared and filtered running buffer containing 10 mM HEPES, 150 mM NaCl,

3 mM EDTA, 1 mg/mL BSA, and 0.05% Tween-20 (Amresco Catalog# M147-1L) (HBS-EBT), pH7.4 at 25°C and the samples were dispensed in 384-tilted well plates.

Kinetic assays were performed by first capturing mAb using anti-human Fc (AHC) Octet biosensors followed by at least two baseline steps of 30 seconds each in HBS-EBT buffer. The mAb-captured biosensors were then submerged in wells containing different concentrations of antigen for 4-6 minutes followed by 10-15 minutes of dissociation time in HBS-EBT buffer. The mAb-captured sensors were also dipped in wells containing HBS-EBT buffer to allow single reference subtraction in order to compensate for the natural dissociation of captured mAb. The sample plates were placed on the orbital shaker with the shake speed of 1000 rpm and the binding sensorgrams were collected using the high sensitivity 16-channel detection mode on the Octet HTX biosensor. Unless specified, fresh AHC biosensors were used without any regeneration step.

The SCK assay was performed by dipping mAb-captured AHC biosensors in increasing concentrations of antigen for four minutes with a short two minutes of dissociation in between each antigen concentration followed by a 15 minutes dissociation time in HBS-EBT buffer after dipping in the highest antigen concentration.

2.3. Immobilization of anti-human Fc mAb on Biacore 4000 and MASS-1

The entire CM5 or HCA sensor surface was immobilized with the anti-human Fc mAb using a standard protocol reported previously (6). Briefly, the entire sensor surface was first activated by injecting a 1:1 (v/v) mixture of 400 mM EDC and 100 mM NHS at a flow rate of 10 µL/min for 10 minutes. Monoclonal mouse anti-human Fc mAb (10 µg/mL) prepared in 10 mM sodium acetate, pH5.0 was then injected at a flow rate of 10 µL/min for 10 minutes. Finally, the activated carboxylate groups were blocked by injecting 1 M ethanolamine, pH 8.5 for 7 minutes at a flow rate of 10 µL/min. During the entire immobilization procedure, 10 mM sodium acetate, pH 5.0 was used as running buffer. Finally, the uncoupled residual protein was removed by treating the sensor surface with 10-12 seconds injections of 20 mM phosphoric acid, 8-10 times before performing binding studies.

2.4. Binding studies performed on the Biacore 4000 and MASS-1

All binding studies were performed in freshly prepared, filtered and degassed running buffer containing 10 mM HEPES, 150 mM NaCl, 3 mM EDTA and 0.05% Tween-20 (Bio-Rad Catalog# 1610781) (HBS-ET), pH7.4 at 25°C. Before performing the binding studies, the anti-human Fc mAb immobilized sensor surface was equilibrated with HBS-ET by priming the instrument at least 3-4 times. The mAb was first captured over the anti-human Fc mAb immobilized surface followed by the injection of different concentrations of antigen for 4-6 minutes at 30 µL/min. The dissociation of the bound antigen from the mAb surface was later measured for 10-15 minutes in HBS-ET running buffer. At the end of each binding cycle, the mAb capture surfaces were regenerated by injecting 20 mM phosphoric acid for 10-12 seconds. Running buffer without analyte was injected to allow the subtraction of baseline drift resulting from the natural dissociation of captured mAb from the coupled anti-human Fc surface.

2.5. Data processing and analysis of Octet HTX data

The raw data measured on Octet HTX was first exported as text file using the ForteBio data analysis software and was later analyzed using Scrubber fitting model (version 2.0c, BioLogic Software, Campbell, Australia). Binding sensorgrams were first aligned at the beginning of the antigen binding cycle and following the single reference subtraction, binding sensorgrams were globally fit to a 1:1 Langmuir binding model with mass transport limitation. The single reference subtracted SCK data was fitted using SCK binding model with mass transport limitation using the Biacore 3000 BIAevaluation software version 4.1.1. The correlation factor used to evaluate reliability of measured binding rate

constants was calculated by taking the ratio of binding kinetic parameters measured on Biacore 4000 or MASS-1 to those measured using Octet HTX.

2.6. Data processing and analysis of Biacore 4000 and MASS-1 data

Alignment of the raw binding data to the start of the antigen injection along with the single reference subtraction of the binding data generated on the MASS-1 and Biacore 4000 was performed using AnalyserR2 and Biacore 4000 evaluation software, respectively. Single reference subtracted data from both instruments were later exported as text files and analyzed using the Scrubber fitting model (version 2.0c, BioLogic Software, Campbell, Australia), wherein a second reference subtraction using control buffer injections was performed, and the double reference subtracted data were globally fit to a 1:1 Langmuir binding model with mass transport limitation, as reported previously (6,26).

3. RESULTS:

3.1. High density mAb surface exhibits antigen rebinding and affects k_a values on Octet HTX:

Numerous SPR/SPRi based binding studies support the design of kinetics assays using the low density mAb surfaces (6,27,28). However, guidelines on the mAb surface density required to reliably measure binding kinetic values are yet to be established for Octet. We therefore first investigated the effect of mAb surface density on measured rate constants. To extend the scope of this study, five antigens with molecular weights of 20kD, 28kD, 39kD, 48kD, and 68kD were selected. Moreover, based on the existing binding kinetic data previously generated on SPR/SPRi biosensor, a total of 40 mAbs (eight mAbs per antigen) that bound to their respective antigens with a wide range of k_a and k_d values were selected.

All 40 mAbs were first characterized using the TK assay on the Biacore 4000 and MASS-1. Low density mAb was captured using the anti-human Fc immobilized sensor surface followed by the injection of different concentrations of antigen. Representative real time binding sensorgrams for two representative mAbs per antigen are shown in **Figure 1** and the results of the kinetic analysis are provided in **Table 1**. The K_D values of the mAb panel selected in this study ranged from 176 pM to 320 nM (**Supplementary Table I**). Most of the measured kinetic values were within two-fold of each other and the mean ratio of the k_a and k_d values measured on Biacore 4000 to MASS-1 for all 40 mAbs characterized in the study were 0.9 and 1.4, respectively. This indicates that comparable k_a values were measured on both platforms, while the k_d values measured on MASS-1 were approximately 1.4-fold lower than Biacore 4000, as reported previously (6). However, we did observe three outliers in this study and more than two-fold difference in the kinetic values were measured between the two biosensors – (i) k_d value of mAb-6 for 28kD antigen; (ii) k_d and K_D values of mAb-2 for 68kD antigen; and (iii) K_D value of mAb-4 for 68kD antigen (**Supplementary Table I**). The comparability of the k_a, k_d and K_D values determined using the two biosensors was further assessed using the regression statistical analysis and the results yielded R^2 values greater than 0.95. Moreover, the slope of the trend lines for k_a, k_d and K_D correlation plots were found to be around 1 (**Supplementary Figure 1**); which further validated a good correlation in the kinetic values determined on Biacore 4000 and MASS-1.

The effect of the mAb surface density on the values of binding rate constants was later studied on the Octet HTX biosensor. The highest antigen concentration used to fit real time binding curves generated on Biacore 4000 or MASS-1 was selected for designing kinetic assays on Octet HTX. Different densities of mAb (ranging from 0.13 nm to 1.28 nm) were captured on AHC Octet biosensors by varying the mAb concentration and/or capture time. **Figure 1** provides representative mAb-antigen interactions characterized at varying mAb surface densities and the measured binding rate constants are provided in **Table 1**. These representative mAbs were selected based on the largest deviation in the kinetic values observed between Octet HTX and Biacore 4000/MASS-1 biosensor. An artifact in the binding signal was observed during the dissociation phase at higher density surfaces of mAb-2 to 28kD antigen (**Figure 1B**)

and mAb-1 to 39kD antigen (**Figure 1C**). The initial one minute of the dissociation curve was used to fit the data for the 28kD antigen, and hence the fitting model generated similar k_d values for all four mAb surface densities. However, the binding sensorgrams illustrate that at the lower two surface densities (0.22 nm and 0.43 nm), the 28kD antigen completely dissociated from mAb-2 within four minutes of the dissociation phase, but the same interaction failed to achieve complete dissociation for mAb density greater than 0.6 nm. Furthermore, the residuals (difference between the fitted data and the real binding data) were observed to increase with increasing mAb surface density (data not shown), further supporting that the antigen rebinding is linked to the mAb capture level. Similarly, the first three minutes of the dissociation phase was utilized during the analysis of mAb-1 to 39kD antigen, and although comparable k_d values were measured, antigen rebinding was observed at mAb surface densities of 0.66 nm and 1 nm.

The reliability of the kinetic values measured at different mAb surface densities on Octet HTX was also evaluated by calculating the correlation factor (ratio of kinetic values measured on Biacore 4000 or MASS-1 to those generated on Octet HTX). **Figure 2** provides plot of the correlation factor for four representative mAbs per antigen. In this study, K_D values measured on Octet HTX and MASS-1 showed a better concordance compared to Biacore 4000. This was clearly evident in the case of the 48kD (**Figure 2D**) and 68kD (**Figure 2E**) antigens, where a correlation factor of approximately one was observed. Since the artifact in the dissociation curve caused due to antigen rebinding was not considered during the analysis, we did not observe any correlation between the k_d value and mAb surface density. Similar correlation profile was observed for the k_a values measured for 20kD, 39kD, 48kD and 68kD antigens. However, we observed that the k_a values measured for all four mAbs to 28kD antigen was affected by the mAb capture density and was found to be directly proportional to the k_a correlation factor (**Figure 2B**). Higher mAb capture density yielded lower k_a values on the Octet HTX. Binding studies performed using surface densities of less than 0.6 nm generated k_a values within two-fold of Biacore 4000 and MASS-1. However, larger discrepancy was observed in the k_a values for kinetic data generated using higher density mAb surfaces. For example, in comparison to the k_a value generated using Biacore 4000, more than five-fold lower k_a value was measured for mAb-4 captured at 1.2 nm density on Octet HTX. Although we report results of just single experiment in this embodiment, two independent assays were performed on Octet HTX to understand the effect of mAb surface density and similar binding profiles were observed in both experiments.

It is known that high affinity mAb-antigen interactions exhibiting k_a value greater than $10^6\ M^{-1}s^{-1}$ are typically limited by mass transport at higher density mAb surfaces. This typically results in the measurement of slower apparent k_a value, mainly due to the limited transport of antigen to the mAb surface (6). Among 40 mAbs included in this study, only these four mAbs bound to 28kD antigen with k_a value greater than $10^6\ M^{-1}s^{-1}$. We therefore believe that the observed trend in reduced k_a value with increasing mAb surface density is the result of MTL. We understand that single concentration fit is not sufficient to conclusively interpret the interaction to be limited by mass transport and further studies would be required to better understand the observed trend. However, since this study was primarily focused on the identification of appropriate mAb surface density to perform kinetic assays, understanding the trend in k_a profile was beyond the scope of this work. Collectively, based on the association and dissociation profiles observed for 40 mAbs, this study indicated that mAb capture density of less than 0.6 nm is best suited for the measurement of mAb-antigen interaction with affinities ranging from 200 pM to 300 nM.

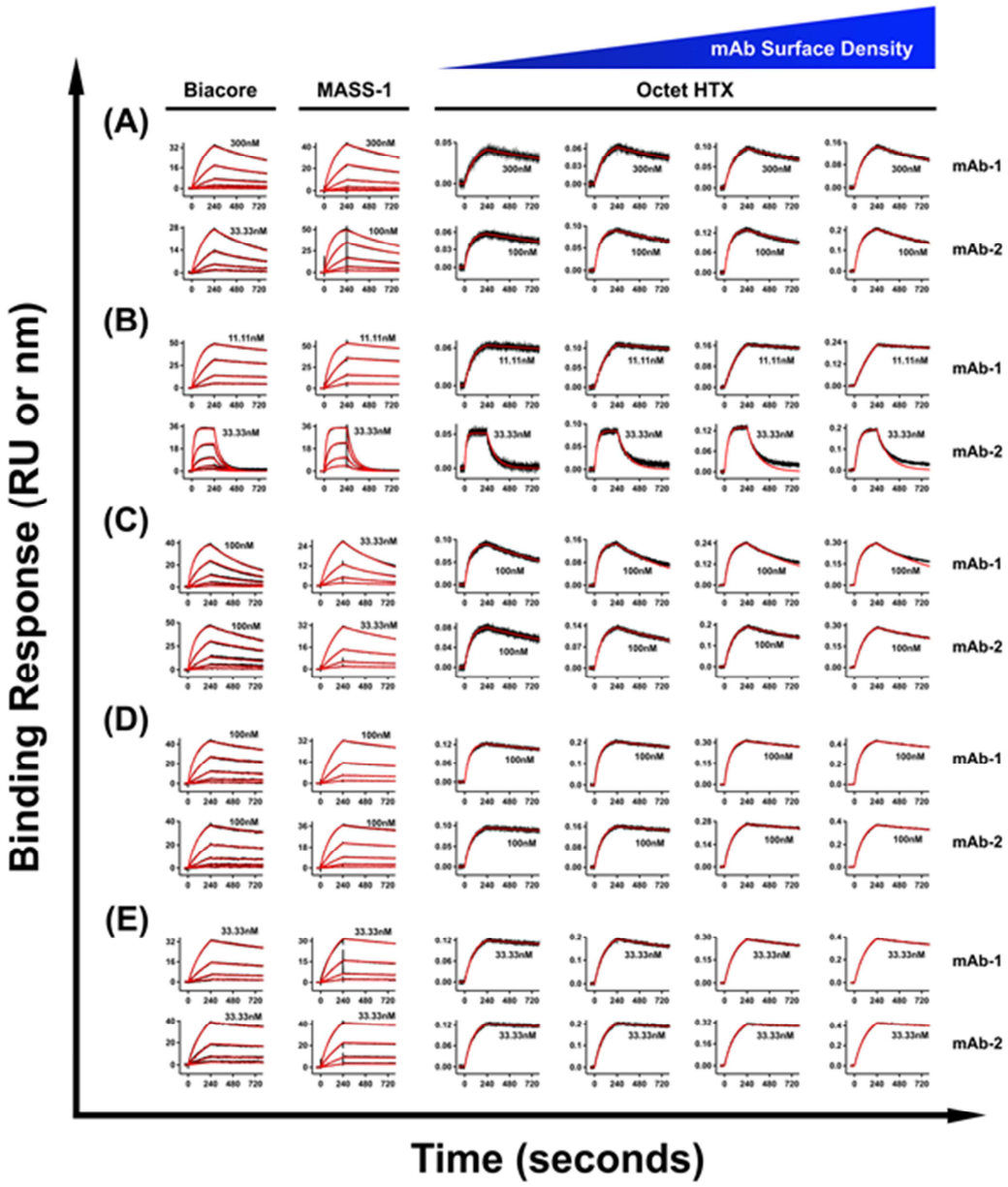

Figure 1: Representative binding sensorgrams showing the effect of mAb surface density on antigen binding on the Octet HTX

The kinetics of mAb binding to 20kD (**A**), 28kD (**B**), 39kD (**C**), 48kD (**D**), and 68kD (**E**) antigen was first measured using Biacore 4000 and MASS-1 by capturing the mAb over the anti-human Fc immobilized CM5 (Biacore 4000) or HCA (MASS-1) sensor chip followed by the injection of different concentrations of antigen (serially diluted by three-fold in HBS-ET buffer). Duplicate injections of the same antigen concentration showed a good overlap and the highest concentration used to fit the binding curves are also provided. The effect of mAb surface density was later studied on Octet HTX by first capturing different densities of mAb on the AHC Octet sensors followed by dipping the AHC sensors in wells containing indicated concentration of antigen. Single reference subtraction of Octet data was performed by dipping mAb captured AHC sensors in HBS-EBT buffer to correct for the natural dissociation of captured mAb from the AHC sensors. Two independent experiments were performed on Octet HTX and representative binding sensorgrams are presented. The real time binding curves are shown as black lines while the red lines indicate the global fits generated by fitting the black line using 1:1 Langmuir binding model with mass transport limitation using the Scrubber software.

Table 1: Binding kinetic parameters from kinetics assays performed using different capture densities of mAb on Octet HTX

Antigen Molecular Weight	mAb Captured	Biacore 4000			MASS-1			Octet HTX													
		k_a (1/Ms)	k_d (1/s)	K_D (M)	k_a (1/Ms)	k_d (1/s)	K_D (M)	Capture Level (nm)	k_a (1/Ms)	k_d (1/s)	K_D (M)	Capture Level (nm)	k_a (1/Ms)	k_d (1/s)	K_D (M)	Capture Level (nm)	k_a (1/Ms)	k_d (1/s)	K_D (M)	Capture Level (nm)	k_a (1/Ms)	k_d (1/s)	K_D (M)
20kD	mAb-1	2.52×10^4	7.57×10^{-4}	3.00×10^{-8}	2.77×10^4	6.23×10^{-4}	2.25×10^{-8}	0.17	2.73×10^4	5.55×10^{-4}	2.04×10^{-8}	0.32	3.10×10^4	6.58×10^{-4}	2.12×10^{-8}	0.54	3.08×10^4	6.33×10^{-4}	2.05×10^{-8}	0.95	3.02×10^4	7.37×10^{-4}	2.44×10^{-8}
	mAb-2	1.96×10^5	1.23×10^{-3}	6.25×10^{-9}	1.59×10^5	8.53×10^{-4}	5.38×10^{-9}	0.22	1.75×10^5	4.75×10^{-4}	2.72×10^{-9}	0.42	1.82×10^5	5.75×10^{-4}	3.17×10^{-9}	0.70	1.76×10^5	6.73×10^{-4}	3.82×10^{-9}	1.22	1.46×10^5	7.27×10^{-4}	4.97×10^{-9}
28kD	mAb-1	1.04×10^6	2.73×10^{-4}	2.62×10^{-10}	1.18×10^6	2.07×10^{-4}	1.76×10^{-10}	0.20	1.03×10^6	1.60×10^{-4}	1.55×10^{-10}	0.37	6.28×10^5	1.97×10^{-4}	3.14×10^{-10}	0.60	7.73×10^5	1.81×10^{-4}	2.34×10^{-10}	1.00	3.21×10^5	1.38×10^{-4}	4.30×10^{-10}
	mAb-2	1.51×10^6	1.88×10^{-2}	1.24×10^{-8}	1.39×10^6	1.58×10^{-2}	1.13×10^{-8}	0.22	1.78×10^6	1.21×10^{-2}	6.77×10^{-9}	0.43	8.84×10^5	9.35×10^{-3}	1.06×10^{-8}	0.68	7.71×10^5	9.52×10^{-3}	1.23×10^{-8}	1.12	5.25×10^5	8.65×10^{-3}	1.65×10^{-8}
39kD	mAb-1	1.27×10^5	1.69×10^{-3}	1.33×10^{-8}	1.81×10^5	1.55×10^{-3}	8.59×10^{-9}	0.20	1.66×10^5	9.42×10^{-4}	5.67×10^{-9}	0.38	1.97×10^5	1.56×10^{-3}	7.93×10^{-9}	0.66	1.65×10^5	1.37×10^{-3}	8.29×10^{-9}	1.01	1.48×10^5	1.39×10^{-3}	9.40×10^{-9}
	mAb-2	1.32×10^5	7.27×10^{-4}	5.52×10^{-9}	1.56×10^5	6.05×10^{-4}	3.88×10^{-9}	0.18	1.50×10^5	6.34×10^{-4}	4.23×10^{-9}	0.34	1.24×10^5	6.79×10^{-4}	5.47×10^{-9}	0.55	1.03×10^5	5.71×10^{-4}	5.54×10^{-9}	0.91	8.64×10^4	5.49×10^{-4}	6.35×10^{-9}
48kD	mAb-1	8.46×10^4	3.11×10^{-4}	3.68×10^{-9}	9.60×10^4	2.18×10^{-4}	2.27×10^{-9}	0.21	1.34×10^5	1.24×10^{-4}	9.26×10^{-10}	0.38	1.26×10^5	1.75×10^{-4}	1.38×10^{-9}	0.68	1.16×10^5	1.70×10^{-4}	1.46×10^{-9}	1.17	1.04×10^5	2.00×10^{-4}	1.93×10^{-9}
	mAb-2	1.14×10^5	4.09×10^{-4}	3.58×10^{-9}	1.62×10^5	3.04×10^{-4}	1.88×10^{-9}	0.24	2.00×10^5	2.63×10^{-4}	1.32×10^{-9}	0.42	1.90×10^5	2.32×10^{-4}	1.22×10^{-9}	0.68	1.73×10^5	2.53×10^{-4}	1.46×10^{-9}	1.09	1.57×10^5	2.64×10^{-4}	1.68×10^{-9}
68kD	mAb-1	1.48×10^5	3.34×10^{-4}	2.26×10^{-9}	1.80×10^5	2.22×10^{-4}	1.23×10^{-9}	0.22	2.92×10^5	1.65×10^{-4}	5.66×10^{-10}	0.40	2.66×10^5	3.36×10^{-4}	1.26×10^{-9}	0.65	2.45×10^5	2.86×10^{-4}	1.17×10^{-9}	1.08	2.14×10^5	2.68×10^{-4}	1.25×10^{-9}
	mAb-2	1.73×10^5	2.19×10^{-4}	1.27×10^{-9}	2.39×10^5	7.45×10^{-5}	3.12×10^{-10}	0.21	3.27×10^5	9.05×10^{-5}	2.79×10^{-10}	0.37	2.97×10^5	1.32×10^{-4}	4.44×10^{-10}	0.62	2.57×10^5	8.04×10^{-5}	3.11×10^{-10}	1.04	2.24×10^5	1.16×10^{-4}	5.18×10^{-10}

The results of the kinetic analysis performed on representative mAbs binding to different molecular weight antigens are provided. Kinetic assay on the Octet HTX was performed by capturing mAb at different densities as provided in the table.

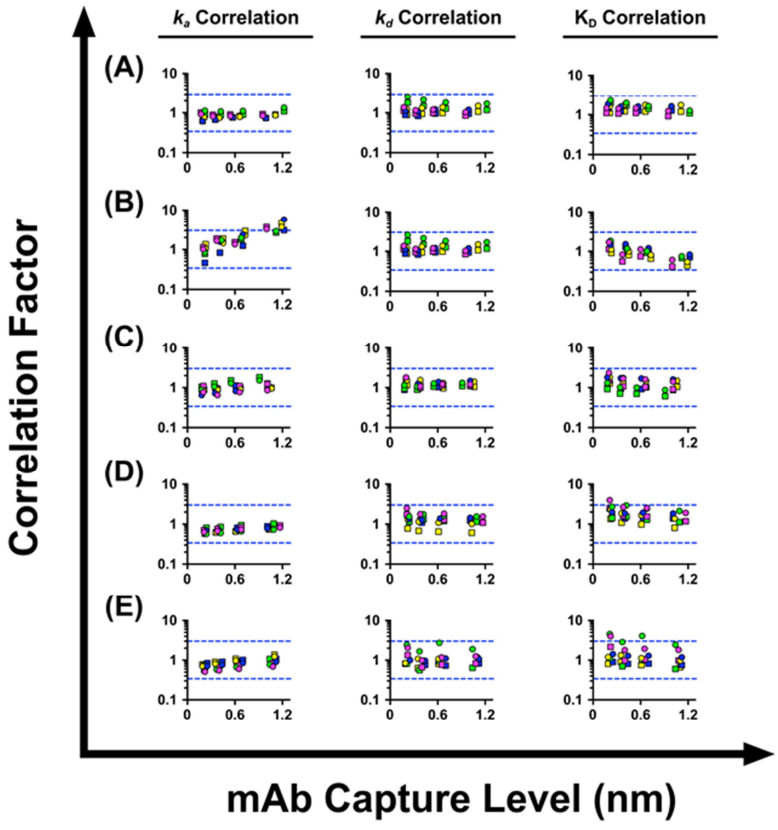

Figure 2: Representative plot of correlation factor showing the fold difference in binding kinetic parameters measured using different capture densities of mAb on Octet HTX

The effect of mAb surface density on the measurement of binding kinetic values on Octet HTX was assessed by plotting the correlation factor against the mAb capture density. The correlation factor was determined by calculating the ratio of k_a, k_d and K_D values measured on Biacore 4000 (circle) or MASS-1 (square) to those measured on Octet HTX at varying mAb surface

densities. Representative correlation factor for mAb-1 (magenta), mAb-2 (green), mAb-3 (blue), and mAb-4 (yellow) binding to 20kD (**A**), 28kD (**B**), 39kD (**C**), 48kD (**D**), and 68kD (**E**) is shown. The blue serrated lines represent correlation factor of three.

3.2. Kinetic analysis performed on Octet HTX are comparable to Biacore 4000 and MASS-1:

Following the identification of optimal mAb surface density, mAb kinetic analysis was performed on Octet HTX using multiple antigen concentrations. A total of 15 mAbs were selected in this study: three mAbs per antigen with molecular weights of 14kD, 29kD, 48kD, 68kD and 105kD. Apart from the standard TK assay, we also attempted to develop SCK assay to characterize mAb-antigen interactions. The SCK assay is a pre-defined injection type on Biacore T200, Biacore X100, Biacore S200 and Biacore 8K and allows the characterization of protein-protein interaction without the need to regenerate the sensor surface (21). We therefore investigated the ability of the Octet biosensor to design a SCK assay to characterize mAb-antigen interactions. The same set of mAbs was also characterized on Biacore 4000 and MASS-1 using the TK assay. **Figure 3** provides representative mAb-antigen interactions for different molecular weight antigens along with the highest antigen concentration used to fit the binding curves. Binding of duplicate antigen concentrations showed good overlap suggesting that reproducible binding data can be generated on Octet HTX irrespective of the assay format (TK or SCK). Moreover, the fitted data perfectly overlapped with the black lines indicating that the fitting model successfully generated global fits using 1:1 Langmuir binding model with mass transport limitation. Average k_a, k_d and K_D values generated from at least three independent experiments performed on different biosensors ranged from 150 pM to 40 nM (**Table 2**). The binding kinetic parameters measured from different biosensors were compared using the linear regression fits. As expected, a high degree of correlation was observed between Biacore 4000 and MASS-1 as manifested by the R^2 values close to 1, while the trendline slope of 1 supports the comparability of kinetic values measured on Biacore 4000 and MASS-1 (**Supplementary Figure 2**). Similarly, the kinetic values measured on Octet HTX correlated with those generated using Biacore 4000 and MASS-1 as evident by the R^2 values of around 1 (**Figure 4**). We also did not observe any trend in the binding rate constants measured on Octet HTX and all the values were found to be randomly distributed. The slope of the trend lines for the k_a, k_d, and K_D correlation plots was close to 1, indicating that the kinetic values measured on Octet HTX were in excellent agreement with those generated using Biacore 4000 and MASS1. In comparison to the k_a values measured on MASS-1 (R^2 = 0.81), the k_a values generated on Octet HTX exhibited better correlation with Biacore 4000 (R^2 = 0.92). The important feature of this study is the high degree of correlation between the binding kinetic parameters measured using TK and SCK assays on Octet HTX (**Figure 4**). The binding rate constants generated using the SCK assay also correlated with the MASS-1 and Biacore 4000 data (**Supplementary Figure 3**).

The experiment to experiment variability of the kinetic analysis performed on different biosensors was also assessed by plotting the binding affinity isotherm (plot of k_a vs. k_d) as shown in **Figure 5**. These plots reveal the experimental spread in the rate constants determined from replicate studies and in turn shed light on the reproducibility of the measured k_a and k_d values. Irrespective of the biosensor or the assay format used to characterize mAb-antigen interactions, minimal variability in the k_a and k_d values was observed and the kinetic values measured from multiple experiments clustered together. Only one outlier was observed in the k_a value measured on Biacore 4000 for mAb-1 binding to 29kD antigen (**Figure 5B**). Overall, the reproducibility of the kinetic values measured on the Octet biosensor was observed to be similar to Biacore 4000 and MASS-1 and the average error in the k_a, k_d and K_D values was observed to be less than 30%, 20% and 30%, respectively.

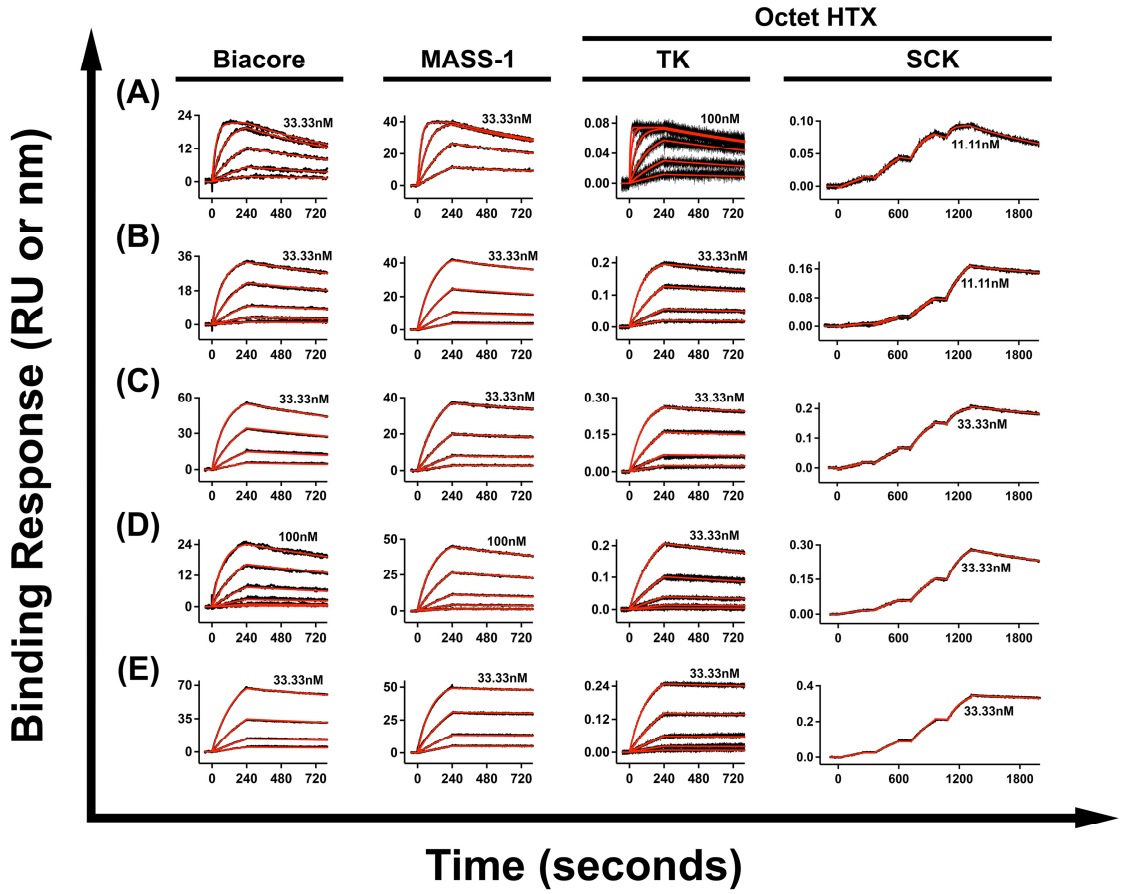

Figure 3: Representative binding sensorgrams for mAb-antigen interactions using titration kinetic (TK) and single cycle kinetic (SCK) assay formats

The mAb was first captured using AHC sensors on Octet HTX or using anti-human Fc immobilized CM5 (Biacore 4000) or HCA (MASS-1) sensor chip followed by dipping in (Octet HTX) or injection of (Biacore 4000 or MASS-1) different concentrations of antigen, serially diluted by three-fold in HBS-EBT or HBS-ET buffer respectively. The TK and SCK assay formats were performed on Octet HTX while the TK assay was performed on Biacore 4000 and MASS-1. Real time binding sensorgrams for mAb binding to 14kD (**A**), 29kD (**B**), 48kD (**C**), 68kD (**D**), and 105kD (**E**) antigen are shown in black and global fits obtained using 1:1 Langmuir binding model with mass transport limitation is represented by red lines. Binding sensorgrams generated using SCK assay format on Octet HTX is provided in the last panel. The results of the kinetic analysis are tabulated in **Table 2**.

Table 2: Binding kinetic parameters for mAb-antigen interactions using titration kinetic (TK) and single cycle kinetic (SCK) assay formats

		Biacore 4000			MASS-1			Octet HTX					
		Titration Kinetic (TK)						Titration Kinetic (TK)			Single Cycle Kinetic		
Antigen Molecular Weight	mAb Captured	k_a ($x10^5$ 1/Ms)	k_d ($x10^{-4}$ 1/s)	K_D ($x10^{-9}$ M)	k_a ($x10^5$ 1/Ms)	k_d ($x10^{-4}$ 1/s)	K_D ($x10^{-9}$ M)	k_a ($x10^5$ 1/Ms)	k_d ($x10^{-4}$ 1/s)	K_D ($x10^{-9}$ M)	k_a ($x10^5$ 1/Ms)	k_d ($x10^{-4}$ 1/s)	K_D ($x10^{-9}$ M)
14kD	mAb-1	14.79 ± 2.07	6.82 ± 1.03	0.48 ± 0.16	12.57 ± 3.66	5.27 ± 0.50	0.44 ± 0.12	19.14 ± 2.00	4.69 ± 1.65	0.25 ± 0.11	18.50 ± 0.46	6.36 ± 1.65	0.34 ± 0.08
	mAb-2	6.88 ± 1.16	76.29 ± 13.15	11.67 ± 4.62	5.82 ± 1.12	73.84 ± 10.34	12.84 ± 1.39	6.35 ± 2.11	67.28 ± 2.72	11.65 ± 4.49	6.76 ± 0.62	61.00 ± 13.97	8.96 ± 1.38
	mAb-3	9.29 ± 1.85	2.06 ± 0.14	0.23 ± 0.06	7.77 ± 0.97	1.74 ± 0.14	0.23 ± 0.05	11.54 ± 1.82	2.43 ± 1.14	0.21 ± 0.08	12.47 ± 0.59	1.85 ± 0.66	0.15 ± 0.05
29kD	mAb-4	3.55 ± 0.71	4.13 ± 0.57	1.23 ± 0.46	4.40 ± 1.09	2.64 ± 0.35	0.64 ± 0.21	3.58 ± 0.17	2.16 ± 0.47	0.60 ± 0.12	4.58 ± 1.45	1.79 ± 0.35	0.44 ± 0.19
	mAb-5	0.32 ± 0.13	3.31 ± 0.43	11.77 ± 4.86	0.48 ± 0.22	2.58 ± 0.38	6.42 ± 3.42	0.37 ± 0.03	2.06 ± 0.37	5.51 ± 0.57	0.54 ± 0.06	2.11 ± 0.30	3.90 ± 0.47
	mAb-6	9.95 ± 2.05	3.55 ± 0.17	0.37 ± 0.10	10.58 ± 2.71	2.95 ± 0.31	0.30 ± 0.10	5.43 ± 0.89	2.47 ± 0.19	0.46 ± 0.04	6.05 ± 1.15	2.86 ± 0.88	0.47 ± 0.12
48kD	mAb-7	3.6 ± 0.18	3.47 ± 0.49	0.97 ± 0.18	3.09 ± 0.54	2.02 ± 0.24	0.66 ± 0.06	3.30 ± 0.22	1.87 ± 0.71	0.56 ± 0.21	3.63 ± 0.41	2.20 ± 0.51	0.60 ± 0.11
	mAb-8	2.67 ± 0.38	11.29 ± 2.55	4.28 ± 1.08	2.46 ± 0.60	7.54 ± 0.18	3.26 ± 1.03	3.04 ± 0.54	6.57 ± 1.08	2.25 ± 0.72	2.86 ± 0.19	9.40 ± 2.83	3.26 ± 0.80
	mAb-9	1.71 ± 0.21	10.05 ± 1.16	5.98 ± 1.30	1.84 ± 0.45	7.45 ± 0.21	4.28 ± 1.29	2.46 ± 0.36	5.98 ± 0.67	2.45 ± 0.35	2.82 ± 0.50	7.21 ± 1.61	2.55 ± 0.25
68kD	mAb-10	1.37 ± 0.14	4.1 ± 0.12	3.02 ± 0.29	1.52 ± 0.36	2.81 ± 0.07	1.95 ± 0.55	2.00 ± 0.31	2.33 ± 0.55	1.21 ± 0.43	1.81 ± 0.35	3.59 ± 1.20	1.95 ± 0.39
	mAb-11	2.32 ± 0.27	11.28 ± 1.97	4.92 ± 1.04	2.23 ± 0.50	7.53 ± 0.03	3.54 ± 0.98	2.80 ± 0.16	6.90 ± 0.32	2.46 ± 0.09	2.99 ± 0.36	8.14 ± 2.50	2.71 ± 0.64
	mAb-12	2.52 ± 0.43	1.79 ± 0.12	0.72 ± 0.10	2.02 ± 0.43	0.84 ± 0.23	0.41 ± 0.04	2.10 ± 0.21	0.71 ± 0.02	0.34 ± 0.04	1.86 ± 0.08	0.72 ± 0.10	0.39 ± 0.07
105kD	mAb-13	2.05 ± 0.13	1.56 ± 0.39	0.76 ± 0.21	2.62 ± 0.58	1.25 ± 0.62	0.50 ± 0.25	2.58 ± 0.14	0.70 ± 0.01	0.27 ± 0.01	2.28 ± 0.03	0.68 ± 0.08	0.30 ± 0.04
	mAb-14	3.11 ± 0.48	127.86 ± 24.43	41.38 ± 7.74	4.84 ± 1.85	86.45 ± 7.77	19.53 ± 5.98	2.78 ± 0.40	81.00 ± 9.37	29.97 ± 8.34	3.78 ± 0.78	65.60 ± 1.87	18.00 ± 4.78
	mAb-15	2.01 ± 1.04	16.30 ± 1.83	10.40 ± 6.09	4.20 ± 2.37	13.73 ± 1.89	4.07 ± 2.00	1.44 ± 0.27	13.39 ± 1.85	9.76 ± 3.50	1.62 ± 0.13	11.00 ± 0.61	6.81 ± 0.89

Results of the kinetic analysis performed on Biacore 4000, MASS-1 and Octet HTX is provided. The values represent average of at least three independent experiments (± standard deviation) performed on 15 mAbs using TK or SCK assay formats.

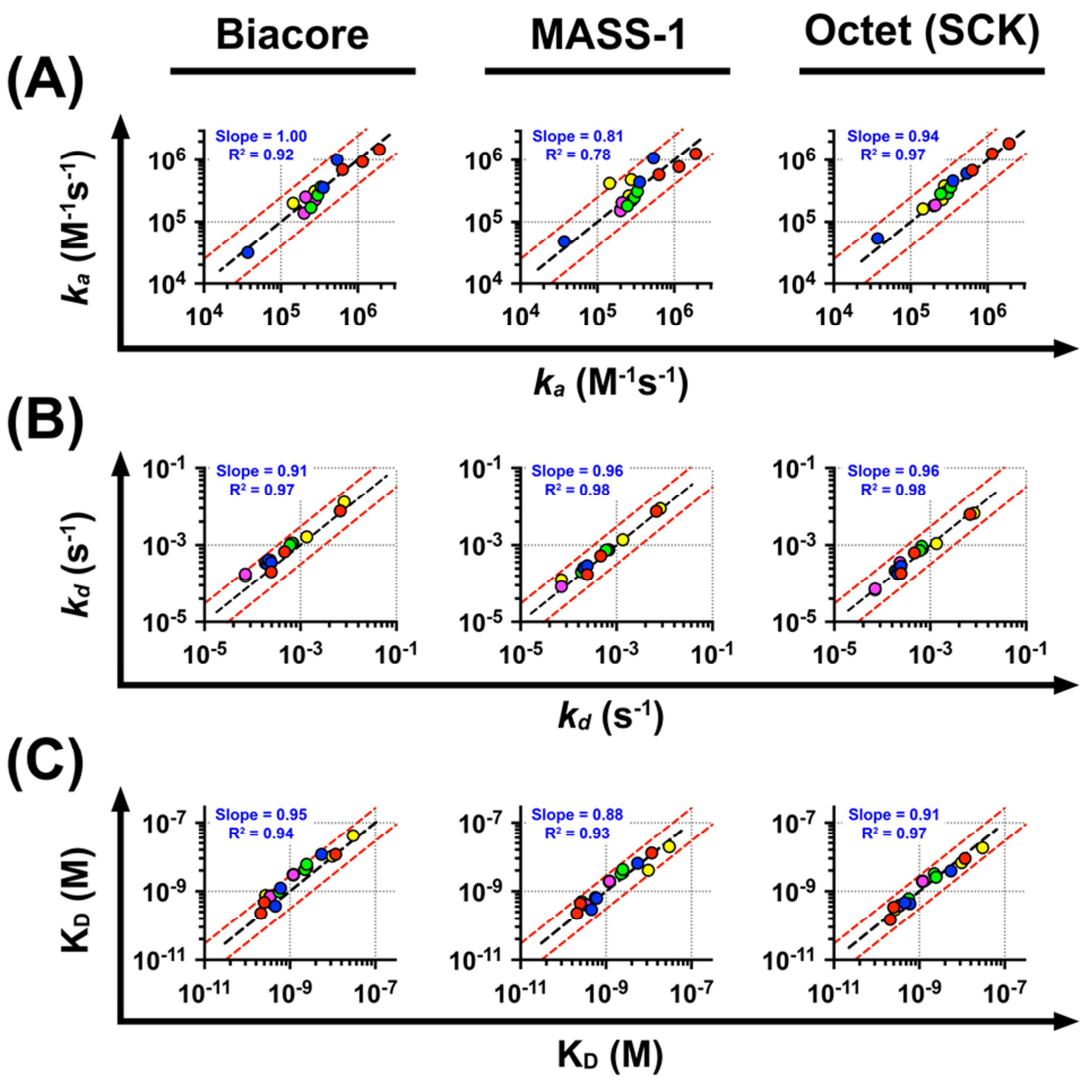

Figure 4: Correlation of the binding kinetic values generated using titration kinetic (TK) and single cycle kinetic (SCK) assays

Graphical representation showing the correlation of average values of k_a (**A**), k_d (**B**) and K_D (**C**) determined from at least three independent experiments measured for mAbs binding to 14kD (●), 29kD (●), 48kD (●), 68kD (●), or 105kD (●) antigen. The kinetic values calculated using the TK assay on Octet HTX is plotted on the X-axis while the binding kinetic parameters measured using TK assay on Biacore 4000, MASS-1 or using SCK assay on Octet HTX is plotted on the Y-axis. The scatter plots were fit using a linear regression fit in excel and the slope of the trend line (black serrated line) along with the correlation coefficients (R^2) is shown in the plot. The two serrated red lines represent three-fold difference in the measured values.

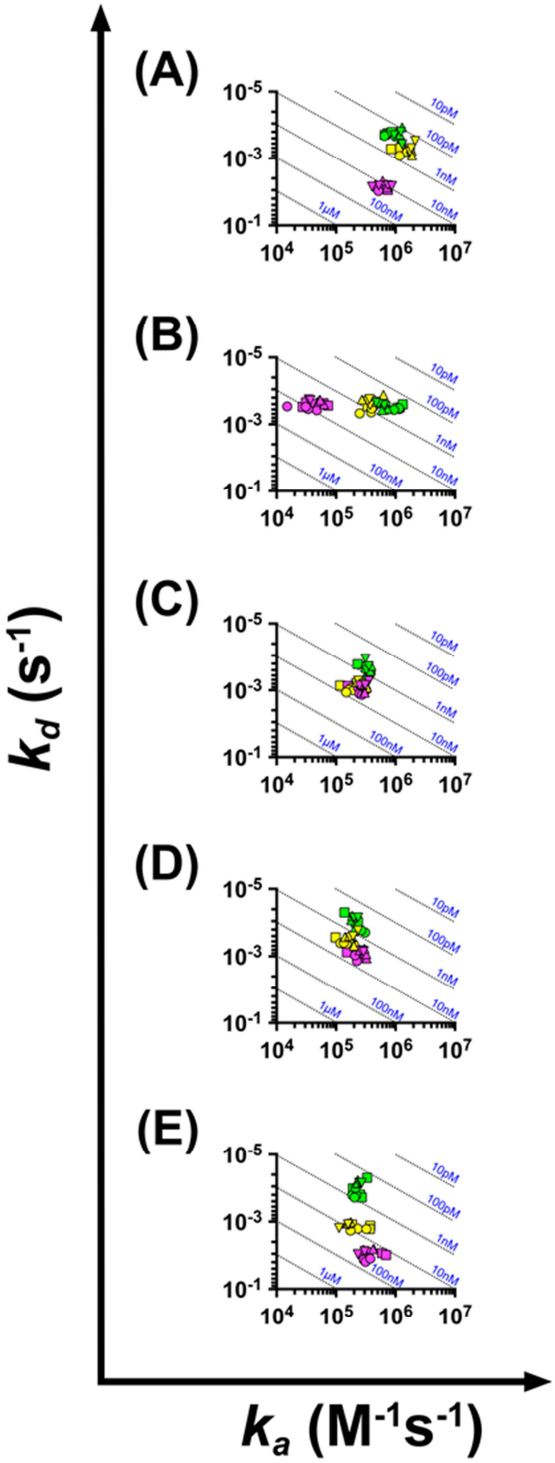

Figure 5: Binding affinity isotherm showing reproducibility of binding kinetic values measured on different biosensors

Graphical representation of k_a versus k_d values generated from individual experiments using TK assay format on Biacore 4000 (circle), MASS-1 (square), Octet HTX (inverted triangle) or SCK assay format on Octet HTX (triangle) to characterize 14kD (**A**), 29kD (**B**), 48kD (**C**), 68kD (**D**), or 105kD (**E**) antigen binding to mAb-1 (magenta), mAb-2 (yellow) or mAb-3 (green). The

binding affinity isotherm plots also provide experimental spread in the binding rate constants using TK and SCK assays. The dotted diagonal lines represent isoaffinity lines along with the respective affinity values.

3.3. Characterization of picomolar affinity mAb-antigen interactions exhibiting k_a values greater than 10^6 $M^{-1}s^{-1}$

Unlike the continuous flow RT-LF biosensors such as Biacore 4000 and MASS-1 wherein samples are injected through a microfluidic device at a high flow rate, the sample plates used in Octet biosensors are placed on top of an orbital shaker (typically set at the shake speed of 1000 rpm) to ensure that the analyte diffusion is not limited by Brownian motion. However, the shake speed of even 1000 rpm is not high enough to allow characterization of picomolar affinity interactions and the Octet biosensors continue to exhibit challenges such as restricted analyte diffusion, analyte rebinding, and MTL, thus limiting its application for kinetic analysis of picomolar affinity mAb. We have demonstrated that reliable and reproducible binding rate constants can be measured on Octet HTX for binding affinities ranging from 150 pM to 300 nM (**Figure 3**, **Figure 4**, and **Figure 5**). However, we wanted to assess the ability of Octet HTX to characterize mAb-antigen interactions with binding affinities greater than 100 pM, especially with k_a value greater than 10^6 $M^{-1}s^{-1}$. Moreover, we were interested in understanding the challenges involved in designing kinetic assays for such picomolar affinity mAbs that are typically limited by mass transport. Among different strategies available, performing kinetic analysis using reduced mAb surface density is the preferred choice to overcome MTL (6,29,30). Seven picomolar affinity mAbs (labeled as mAb-1 through mAb-7) exhibiting MTL for antigen binding using standard 0.4-0.6 nm mAb surface densities were selected in this study and TK assay was performed on Octet HTX and MASS-1 by capturing mAbs at two densities: (i) standard density, and (ii) ultra-low density. Approximately 0.5 nm or 0.1 nm of mAb was captured on Octet HTX, while on MASS-1 mAbs were captured at varying surface densities depending on the antigen molecular weight as indicated in **Table 3**.

Figure 6 provides binding sensorgrams for seven mAbs characterized in this study along with the highest antigen concentration used to fit the binding curves. The k_a, k_d and K_D values generated by the binding assays performed using both density mAb surfaces on MASS-1 were found to be less than two-fold of each other (**Table 3**). We observed that incorporation of mass transport factor (k_m) in the fitting model was required to fit the binding curves generated using standard density mAb surface and the fits yielded less than 0.3 RU residuals that were randomly distributed (data not shown), which is the characteristic of a good fit. This suggests that the model was able to successfully compensate for the observed MTL. On the other hand, the data generated using ultra-low density mAb surface did not require k_m in the fitting model (data not shown), indicating that the interaction was not limited by mass transport.

In the case of Octet HTX however, MTL was observed for both 0.5 nm and 0.1 nm density surfaces for all seven mAbs characterized in this study. The binding data generated on Octet HTX using the 0.1 nm mAb surface exhibited very poor signal to noise, especially for the mAb to 14kD antigen wherein the noise of the measured binding signal failed to discriminate the spacing between different antigen concentrations. Smoothening of the raw binding signal was required to distinguish the specific signal from instrument noise and also to show the spacing between different antigen concentrations (**Supplementary Figure 4**). The model however, was able to fit the raw binding data (without smoothening) and the values of k_a, k_d and K_D generated by the model are reported in **Table 3**. Kinetic values measured using the 0.1 nm mAb density correlated with the MASS-1 data. Except for mAb-7, the binding affinities measured on Octet HTX were within two-fold of MASS-1 values. The k_d value measured for mAb-7 on Octet HTX was comparable to MASS-1 and the observed three-fold difference in the K_D value was due to the measurement of three-fold lower k_a value.

In comparison to the data generated using the 0.1 nm mAb surfaces, binding studies performed on Octet HTX using 0.5 nm mAb capture density were significantly limited by mass transport. Real time binding

data did not perfectly overlap with the globally fitted data and large non-randomly distributed residuals (greater than 5% of the binding response) were observed during the association phase of mAb-3, mAb-4, mAb-5, mAb-6, and mAb-7 (**Supplementary Figure 5**). Among the seven mAbs studied using 0.5 nm capture density, the k_a, k_d and K_D values of only three mAbs (mAb-1, mAb-2, and mAb-6) were within three-fold of the values generated on MASS-1 (**Table 3**). It is known that the fitting model can successfully compensate for partially limited interaction, but it fails to fit significantly mass transport limited binding curves, thereby yielding erroneous values of binding kinetic parameters, as observed in the case for mAb-3, mAb-4, mAb-5 and mAb-7. The binding rate constants measured for these four mAbs using 0.5 nm mAb surface were more than three-fold different from those measured using MASS-1. The largest error in the kinetic measurement was observed for mAb-5 where the model extrapolated a 10-fold lower k_d value and a 24-fold difference in the K_D values. Collectively, these data strongly support the rationale of designing binding kinetic assays that are devoid of MTL in order to measure reliable kinetic values for any protein-protein interaction.

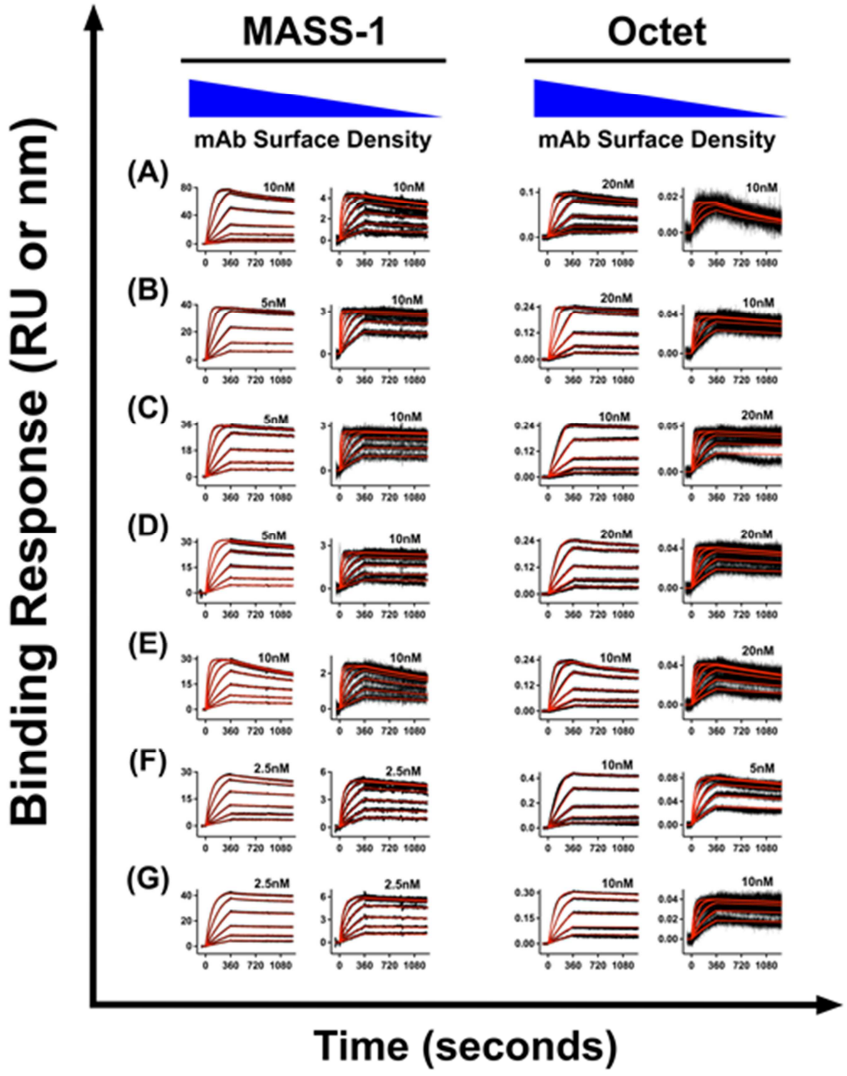

Figure 6: Binding sensorgrams of picomolar affinity mAb-antigen interactions studied using two capture densities of mAb

Standard or ultra-low density of mAb binding to 14kD (**A**), 39kD (**B**, **C**, **D**, **E**) or 71kD (**F, G**) antigen was captured using HCA sensor immobilized with anti-human Fc (MASS-1) or using AHC Octet sensors (Octet HTX). Varying concentrations of antigen (two-fold serial dilution) were injected over different density mAb surfaces for 6 minutes followed by 15 minutes of dissociation. Red lines represent the global fits of the real time binding sensorgrams (black lines) using a 1:1 Langmuir binding model with mass transport limitation. The highest antigen concentration used to fit the data is also shown and the results of the kinetic analysis are tabulated in **Table 3**.

Table 3: Binding kinetic parameters for picomolar affinity mAb-antigen interactions

		MASS-1					Octet HTX				
Antigen Molecular Weight	mAb Captured	Capture Level (RU)	k_m (cm/s)	k_a (1/Ms)	k_d (1/s)	K_D (M)	Capture Level (nm)	k_m (cm/s)	k_a (1/Ms)	k_d (1/s)	K_D (M)
14kD	mAb-1	350	8.57×10^{7}	3.29×10^{6}	3.14×10^{-4}	9.54×10^{-11}	0.60	6.39×10^{4}	3.73×10^{6}	2.92×10^{-4}	7.81×10^{-11}
		19	7.54×10^{9}	4.34×10^{6}	2.46×10^{-4}	5.67×10^{-11}	0.12	1.00×10^{10}	4.92×10^{6}	3.30×10^{-4}	6.70×10^{-11}
39kD	mAb-2	70	1.51×10^{8}	1.30×10^{7}	1.20×10^{-4}	9.21×10^{-12}	0.50	1.43×10^{5}	7.44×10^{6}	1.24×10^{-4}	1.67×10^{-11}
		6	8.36×10^{9}	1.26×10^{7}	8.06×10^{-5}	6.43×10^{-12}	0.11	9.39×10^{4}	2.05×10^{7}	9.85×10^{-5}	4.81×10^{-12}
	mAb-3	59	1.42×10^{8}	8.10×10^{6}	9.85×10^{-5}	1.22×10^{-11}	0.56	1.98×10^{5}	2.63×10^{6}	1.38×10^{-4}	5.24×10^{-11}
		6	5.00×10^{9}	8.09×10^{6}	4.83×10^{-5}	5.93×10^{-12}	0.11	9.29×10^{4}	8.15×10^{6}	5.47×10^{-5}	6.71×10^{-12}
	mAb-4	60	1.99×10^{8}	4.95×10^{6}	1.50×10^{-4}	3.03×10^{-11}	0.53	1.61×10^{5}	2.42×10^{6}	3.42×10^{-4}	1.41×10^{-10}
		6	1.35×10^{9}	4.76×10^{6}	6.26×10^{-5}	1.32×10^{-11}	0.11	1.44×10^{5}	3.83×10^{6}	9.38×10^{-5}	2.45×10^{-11}
	mAb-5	65	2.63×10^{8}	4.46×10^{6}	3.87×10^{-4}	8.67×10^{-11}	0.53	1.04×10^{5}	1.05×10^{7}	3.85×10^{-5}	3.60×10^{-12}
		6	1.00×10^{10}	5.86×10^{6}	3.52×10^{-4}	6.00×10^{-11}	0.11	5.00×10^{6}	3.41×10^{6}	3.29×10^{-4}	9.64×10^{-11}
71kD	mAb-6	32	4.71×10^{8}	6.31×10^{6}	1.50×10^{-4}	2.38×10^{-11}	0.60	2.38×10^{5}	2.80×10^{6}	7.42×10^{-5}	2.65×10^{-11}
		5	1.00×10^{10}	8.21×10^{6}	1.23×10^{-4}	1.50×10^{-11}	0.10	1.00×10^{10}	1.55×10^{7}	1.41×10^{-4}	9.08×10^{-12}
	mAb-7	45	4.44×10^{8}	6.19×10^{6}	7.17×10^{-5}	1.16×10^{-11}	0.40	4.21×10^{5}	1.92×10^{6}	6.10×10^{-5}	3.17×10^{-11}
		6	1.00×10^{10}	7.53×10^{6}	6.88×10^{-5}	9.16×10^{-12}	0.07	1.00×10^{10}	2.81×10^{6}	6.78×10^{-5}	2.41×10^{-11}

The binding data was generated using MASS-1 and Octet HTX by capturing mAbs at two densities as shown in the table. The results of the kinetics analysis for seven picomolar affinity mAbs generated using two densities are provided.

3.4. Binding kinetic parameters measured on a panel of 150 mAbs using Octet HTX are comparable with Biacore 4000 and MASS-1:

During the design of TK assay on the SPR/SPRi biosensors, sensor surfaces are routinely regenerated at the end of each binding cycle to remove the captured mAb. Regeneration enables characterization of a large panel of mAb-antigen interactions using just one biosensor chip. Although using an individual Octet biosensor is more affordable than the SPR/SPRi biosensors, characterization of a panel of around 30 mAbs using a TK assay without regenerating the Octet biosensors can be expensive. We therefore studied the effect of regeneration on the kinetic analysis of mAb-antigen interactions using Octet HTX. A total of 150 human mAbs to 10 antigens with molecular weights ranging from 21kD to 105kD were characterized on Octet HTX using TK assay. The same set of mAbs was characterized earlier on Biacore 4000 and MASS-1 (6) and the previously determined binding kinetic parameters were used to compare the kinetic values generated on Octet HTX in this study. The **Figure 7** provides representative binding sensorgrams for mAb binding to different molecular weight antigens along with the highest antigen concentration used to fit the real time binding sensorgrams (black lines). Average k_a, k_d or K_D values generated from at least three independent experiments (± standard deviation) are listed in **Table 4**. The reproducibility of binding data generated on Octet HTX was evident based on the overlap of duplicate antigen

concentrations, while the global fits (red line) overlapped with the black lines, thus validating the good fits generated by the model.

The **Figure 8** provides scatterplot showing the correlation of the average binding kinetic parameters generated on Octet HTX with those measured on Biacore 4000 and MASS-1. Based on the visual inspection of the correlation plot, we did not observe any significant difference in the k_a, k_d or K_D values measured across different biosensors. No significant experiment-to-experiment variability in the measured binding rate constants was observed across different biosensors and the standard errors in the k_a, k_d and K_D averaged around 20%. The kinetic values were found to be randomly distributed along the diagonal and did not exhibit any trend in the measured k_a, k_d or K_D values across different biosensors as reported previously (28). More than 96% of the k_a and k_d values measured on the Octet HX were within three-fold of the values measured on the Biacore 4000 and MASS-1. Around 94% of the K_D values measured on Octet HTX were within three-fold of values measured on Biacore 4000, while approximately 83% of the K_D values measured on MASS-1 were within three-fold of values measured on Octet HTX. We also performed a linear regression analysis on the complete data set and assessed the slope of the trend line along with the R^2 values (**Figure 8**). The k_a, k_d and K_D values measured on Octet HTX highly correlated with those measured using Biacore 4000 and MASS-1 with R^2 values close to 1. The slope of the trend line for the k_a scatter plot was around 1.36 with the R^2 value of 0.75. The prominent feature of this study was that the k_d and K_D values measured on Octet HTX showed a remarkable correlation with Biacore 4000 and MASS-1 and the R^2 values were observed to be greater than 0.92 and 0.90, respectively Moreover, the slope of the trend lines were found to be close to 1, further supporting that comparable k_d and K_D values were measured across different biosensors. These data further validates that upon optimization of experimental conditions, mAb-antigen binding kinetic values measured on the Octet platform can be comparable to those measured using the well-established SPR/SPRi platforms.

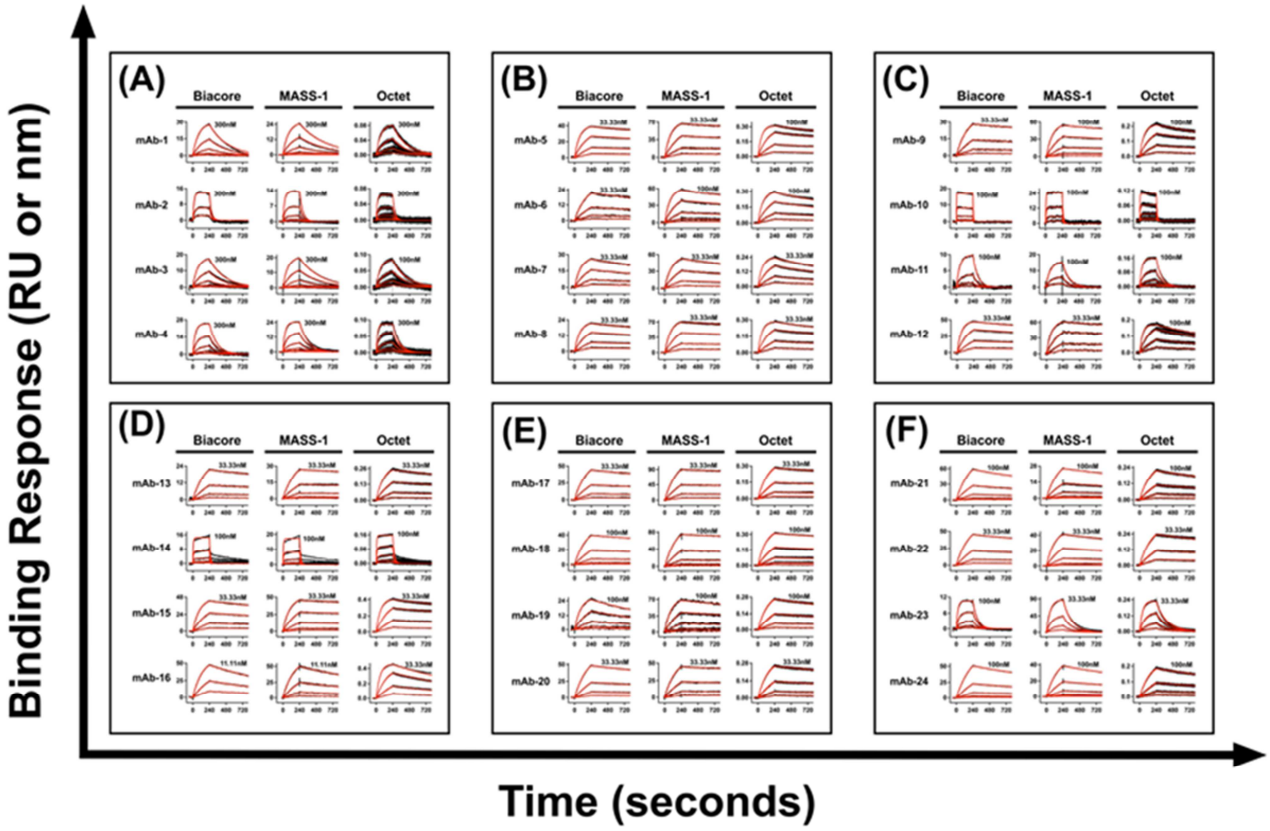

Figure 7: Representative binding sensorgrams from the comparability study performed on Biacore 4000, MASS-1 and Octet HTX biosensors

Titration kinetic assay was performed on Biacore 4000, MASS-1, and Octet HTX by capturing mAb binding to 21kD (**A**), 28kD (**B**), 29kD (**C**), 48kD (**D**), 92kD (**E**), and 105kD (**F**) on an anti-human Fc immobilized CM5 (Biacore 4000) or HCA (MASS-1) or using AHC Octet sensors followed by the binding of different concentrations of antigen. In this study, AHC Octet sensors were regenerated by dipping the AHC sensors in wells containing 20mM phosphoric acid for 20 seconds thrice with neutralization of AHC Octet sensors in HBS-EBT buffer for 20 second in between each dip. The real time binding sensorgrams are shown in black lines while red lines represent the global fits generated by globally fitting the black lines using 1:1 Langmuir binding model with mass transport limitation. The highest concentration used to fit the data is also provided. To ensure that our analysis did not introduce any unintended biasing in the measurement of rate constants, all binding data generated on different biosensors were independently analyzed by adopting the "blind analysis" technique, wherein the antigen concentrations that yielded the best global fits of the reference subtracted data were selected, as reported previously (6). This resulted in the inclusion of different concentration series during the data analysis of few mAb-antigen interactions (**Biacore 4000**: mAb-6, mAb-9, mAb-23; **Octet HTX**: mAb-3, mAb-5, mAb-12, mAb-16). The average values of binding kinetic parameters from at least three independent experiments (± standard deviation) are provided in **Table 4**.

Table 4: Binding kinetic parameters for representative mAb-antigen interactions from the comparability study

Antigen Molecular Weight	mAb Captured	Biacore 4000			MASS-1			Octet HTX		
		k_a ($x10^5$ 1/Ms)	k_d ($x10^{-4}$ 1/s)	K_D ($x10^{-9}$ M)	k_a ($x10^5$ 1/Ms)	k_d ($x10^{-4}$ 1/s)	K_D ($x10^{-9}$ M)	k_a ($x10^5$ 1/Ms)	k_d ($x10^{-4}$ 1/s)	K_D ($x10^{-9}$ M)
21kD	mAb-1	0.33 ± 0.09	35.74 ± 4.27	114.33 ± 38.66	0.39 ± 0.09	25.74 ± 3.91	68.83 ± 21.80	0.33 ± 0.04	53.89 ± 5.52	167.33 ± 41.31
	mAb-2	0.69 ± 0.11	332.47 ± 89.20	478.46 ± 103.81	0.66 ± 0.04	214.33 ± 54.67	321.00 ± 71.51	1.01 ± 0.06	379.57 ± 57.64	378 ± 81.43
	mAb-3	0.42 ± 0.12	39.49 ± 7.83	101.40 ± 40.94	0.44 ± 0.08	30.85 ± 2.36	71.93 ± 16.52	0.58 ± 0.04	50.52 ± 0.50	87.37 ± 5.05
	mAb-4	0.73 ± 0.09	92.83 ± 5.77	127.33 ± 12.66	1.20 ± 0.78	73.48 ± 7.85	76.30 ± 36.63	1.30 ± 0.18	118.43 ± 13.69	91.40 ± 8.27
28kD	mAb-5	4.97 ± 1.70	1.90 ± 0.10	0.41 ± 0.14	3.60 ± 0.22	1.51 ± 0.10	0.42 ± 0.01	2.72 ± 0.30	2.72 ± 0.42	1.00 ± 0.07
	mAb-6	1.82 ± 0.47	3.17 ± 0.13	1.80 ± 0.36	1.20 ± 0.08	3.58 ± 1.01	2.98 ± 0.86	1.78 ± 0.44	5.21 ± 1.55	2.94 ± 0.56
	mAb-7	3.48 ± 0.63	4.24 ± 0.15	1.25 ± 0.24	2.93 ± 0.10	3.82 ± 0.34	1.30 ± 0.07	2.14 ± 0.30	6.15 ± 0.92	2.88 ± 0.27
	mAb-8	5.74 ± 1.81	1.94 ± 0.46	0.38 ± 0.20	3.98 ± 0.40	1.32 ± 0.08	0.33 ± 0.02	2.44 ± 0.54	2.82 ± 0.44	1.17 ± 0.15
29kD	mAb-9	1.97 ± 0.23	2.20 ± 0.30	1.12 ± 0.02	1.44 ± 0.34	1.90 ± 0.14	1.36 ± 0.31	1.95 ± 0.50	3.23 ± 1.62	1.57 ± 0.50
	mAb-10	13.00 ± 3.64	1352.47 ± 465.91	103.43 ± 13.97	10.45 ± 0.69	786.37 ± 51.69	75.57 ± 8.74	5.92 ± 2.85	691.17 ± 325.18	117.67 ± 6.11
	mAb-11	0.62 ± 0.25	151.97 ± 4.38	269.67 ± 92.22	0.68 ± 0.22	101.12 ± 1.53	160.67 ± 59.53	0.75 ± 0.22	112.11 ± 39.51	148.67 ± 22.74
	mAb-12	5.02 ± 1.01	2.16 ± 0.33	0.45 ± 0.16	5.48 ± 1.42	1.59 ± 0.08	0.30 ± 0.07	3.21 ± 0.73	4.83 ± 2.07	1.45 ± 0.34
48kD	mAb-13	1.41 ± 0.17	2.03 ± 0.67	1.44 ± 0.40	1.52 ± 0.23	1.14 ± 0.03	0.76 ± 0.14	1.40 ± 0.06	2.77 ± 0.29	1.99 ± 0.29
	mAb-14	7.58 ± 1.40	744.33 ± 7.37	100.43 ± 18.28	6.63 ± 1.49	598.20 ± 106.82	93.20 ± 27.30	4.91 ± 0.12	482 ± 18.12	98.03 ± 2.67
	mAb-15	3.26 ± 0.21	1.98 ± 0.60	0.61 ± 0.21	3.25 ± 0.01	1.09 ± 0.05	0.34 ± 0.02	2.36 ± 0.13	2.89 ± 0.51	1.23 ± 0.21
	mAb-16	6.16 ± 0.68	6.56 ± 0.83	1.06 ± 0.04	5.65 ± 0.14	5.34 ± 0.06	0.94 ± 0.03	2.99 ± 0.26	6.95 ± 0.76	2.33 ± 0.27
92kD	mAb-17	2.31 ± 0.83	2.73 ± 1.36	1.15 ± 0.20	1.94 ± 0.14	0.79 ± 0.05	0.41 ± 0.06	2.04 ± 0.01	1.48 ± 0.05	0.73 ± 0.02
	mAb-18	0.73 ± 0.22	2.41 ± 1.80	3.05 ± 1.38	0.61 ± 0.04	0.87 ± 0.04	1.44 ± 0.12	1.08 ± 0.39	1.48 ± 0.13	1.50 ± 0.55
	mAb-19	1.55 ± 0.76	6.11 ± 0.94	4.47 ± 1.82	1.41 ± 0.26	2.21 ± 0.13	1.62 ± 0.40	2.16 ± 0.07	2.78 ± 0.19	1.29 ± 0.10
	mAb-20	2.14 ± 0.72	3.12 ± 1.53	1.42 ± 0.26	1.90 ± 0.15	1.03 ± 0.06	0.55 ± 0.07	2.10 ± 0.02	2.08 ± 0.09	0.99 ± 0.04
105kD	mAb-21	0.51 ± 0.04	3.94 ± 0.16	7.70 ± 0.71	0.53 ± 0.09	2.78 ± 0.39	5.28 ± 0.24	0.88 ± 0.04	4.27 ± 0.47	4.89 ± 0.74
	mAb-22	1.53 ± 0.14	2.08 ± 0.24	1.36 ± 0.10	2.21 ± 0.41	2.08 ± 0.59	0.93 ± 0.10	2.04 ± 0.37	2.68 ± 0.47	1.33 ± 0.30
	mAb-23	2.89 ± 0.25	128.82 ± 29.83	44.10 ± 6.73	4.15 ± 1.50	82.76 ± 3.01	21.33 ± 5.84	3.28 ± 0.03	79.42 ± 1.19	24.23 ± 0.35
	mAb-24	2.47 ± 1.45	12.83 ± 0.85	7.46 ± 5.85	3.25 ± 1.69	13.12 ± 1.53	5.02 ± 2.90	1.68 ± 0.33	13.75 ± 0.47	8.35 ± 1.54

The results of the kinetic analysis performed on mAbs shown in **Figure 7**. At least three independent experiments were performed on Biacore 4000, MASS-1 and Octet HTX by first capturing the mAb, followed by the binding of different concentrations of antigen. The sensor surfaces were regenerated at the end of each cycle and average kinetic values (± standard deviation) is provided.

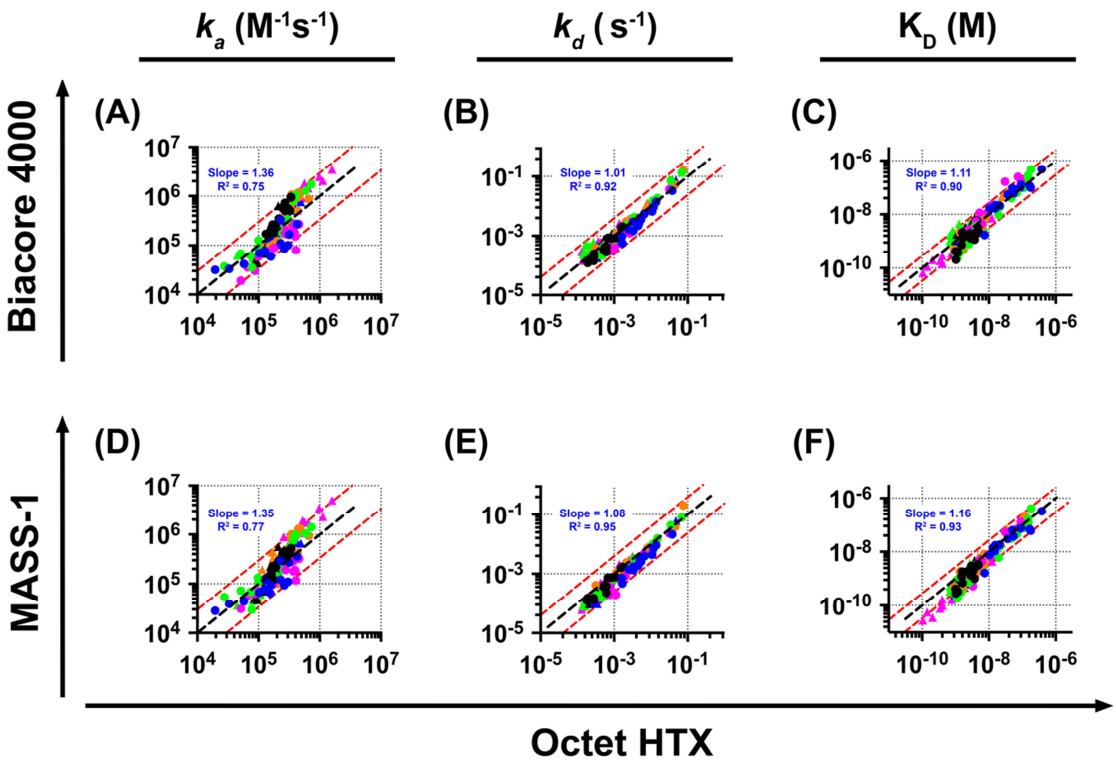

Figure 8: Correlation of the binding kinetic values generated using different biosensors in the comparability study

Graphical representation revealing the correlation of average binding kinetic values measured from at least three independent experiments for 150 mAbs binding to 21kD (●), 28kD (●), 29kD (●), 32kD (●), 38kD (●), 48kD (▲), 68kD (▲), 92kD (▲), 97kD (▲) or 105kD (▲) antigen is shown. The scatterplot of k_a (A, D), k_d (B, E) and K_D (C, F) values calculated using Biacore 4000 (A, B, C) or MASS-1 (D, E, F) was plotted on the y-axis while the values measured using Octet HTX was plotted on the x-axis. The scatter plots were fit using a linear regression fit and the slope of the trend line (black serrated line) along with the correlation coefficients (R^2) is shown in the plot. The two serrated red lines represent three-fold difference in the measured values.

4. DISCUSSION

The Octet biosensor is becoming an important biophysical tool and owing to its ability to support high throughput needs of today's biopharmaceutical industry, Octet biosensors are been widely used in different stages of mAb discovery and development. However, failure to demonstrate reliable measurement of the kinetics of mAb binding to its target antigen has hindered its application for the kinetic screening of mAbs. In an effort to address this problem, we explored different experimental conditions to allow reliable characterization of mAb-antigen interactions on the Octet biosensor. Unlike previous studies that focused on the kinetic analysis of single or multiple mAbs binding to the same antigen (19,20,24,25), in this study we characterized an extensive panel of 165 mAbs binding to 14 different antigens with molecular weights ranging from 14kD to 105kD.

We discovered that the mAb surface density of less than 0.6 nm is essential for reliable measurement of mAb-antigen binding kinetics on Octet HTX. Higher density mAb surfaces resulted in analyte rebinding, which is in agreement with the earlier report (19). A sink method was proposed in the previous study to avoid rebinding, wherein a competing antigen was spiked into the buffer during the dissociation phase. However, this would necessitate the use of a higher affinity competing peptide or antigen, which in turn would require significant time and resources. Moreover, it would be challenging to incorporate this strategy during the kinetic screening of large mAb panel. The data presented in **Figure 1B** (mAb-2) and **Figure 1C** (mAb-1) supports that designing kinetic assays using lower mAb surface density is a better approach to minimize antigen rebinding.

Apart from investigating different experimental conditions such as running buffer, shake speed, and mAb surface density, we also considered various external factors that can potentially influence reliable measurement of mAb-antigen interactions. Since Octet HTX only allows performing binding assays 4°C above the ambient temperature, the room temperature was maintained at around 20°C to perform the binding studies at 25°C reported in this work, similar to the studies described earlier (19). Sample evaporation during the course of the experiment continues to be a challenge for the Octet platform (19,20) and in order to minimize the change in the antigen concentration due to evaporation, the experiment time for most of our Octet assays was limited to less than two hours. Moreover, in order to reduce the influence of user-to-user variability in the measurement of binding kinetic values, all of the data presented in this study was generated and analyzed by a single user. The data presented in this embodiment showcase that upon careful optimization of experimental conditions, Octet biosensors can reliably measure kinetics of mAb-antigen interactions for a wide range of binding affinities. One of the important findings of this study is the validation of the SCK assay on the Octet biosensor (**Figure 3**, **Figure 4**, **Figure 5**, and **Supplementary Figure 3**). Similar to the data generated using the TK assay, the k_a, k_d and K_D values generated using SCK assays on Octet HTX correlated with the values measured on Biacore 4000 (SPR) and MASS-1 (SPRi) biosensors (**Figure 3**, **Figure 4**, **Figure 5**, **Supplementary Figure 3** and **Table 2**).

A wide range of optical biosensors capable of determining kinetics of biomolecular interaction are currently available, each having its own advantages and limitations. As an end user, it is important to understand that the selection of appropriate platform should not only be based on the aim of the study, but also on the strength of the biosensor. Reduced hands-on time, assay time and higher throughput continue to be the biggest advantages of the Octet platform. Starting a new binding assay on SPR/SPRi biosensor typically requires few hours of sensor preparation time – from hydration of the new sensor chip to the immobilization of the appropriate ligand onto the surface. In contrast, a wide range of ready-to-use, pre-immobilized Octet biosensors reduces the sensor preparation time and also provide multiple opportunities to quickly design diverse binding assays on the Octet platform. Pre-equilibrating the Octet biosensors in

the sample buffer for around 15-20 minutes is sufficient for performing kinetic assays. In order to further reduce total hands-on and experiment time, we soak the Octet biosensors in the sample buffer before preparing the samples. Thus, by the time the sample plates are ready for performing the specific binding assay, the biosensors will already be equilibrated in the sample buffer. Pre-immobilizing the SPR/SPRi sensor chip with appropriate capture molecule is a good alternative to reduce sensor preparation time. However, after docking the pre-immobilized sensor chip, the SPR/SPRi biosensor needs to be primed for two to three times in the running buffer to allow equilibration of the sensor surface followed by conditioning of the sensor surface (typically four to five injections of regeneration buffer) and thus will require longer hands-on and preparation time, in comparison to the Octet platform. Moreover, pre-immobilization of the SPR/SPRi sensor chip will require identification of appropriate storage condition to retain the activity of the capture surface, which at times can be challenging. Octet platform thus has an advantage of significantly reduced hands-on time in comparison to the SPR/SPRi biosensors.

Sample recovery after the end of the experiment is another advantage of the Octet platform as opposed to most of the microfluidic based biosensors. This provides an opportunity to repeat the kinetic assay for cases wherein the antigen titration series, ligand surface density, and/or association/dissociation times are not ideal to characterize a particular interaction. However, due to the sample evaporation during the course of the first experiment, the sample concentration might increase and hence the repeat experiment should be designed with this caveat in mind.

Although the Octet platform provides the throughput with reduced experiment time, we experienced a number of challenges in designing kinetic assays. Unlike the SPR/SPRi biosensors that allow characterization of biomolecular interactions over a wide range of temperatures (4-40°C), the Octet biosensors can only perform binding assays with the temperature range of 4°C above the ambient temperature. Less than 10% sample evaporation was typically observed during the two hour experiment performed at 25°C while significant evaporation was observed at 37°C. Samples dispensed in 96-well plate resulted in an approximately 30-35% evaporation in two hours, while less than 18% evaporation was observed during the same time when the samples were dispensed in tilted 384-well plate (data not shown). Therefore, kinetic analysis performed at higher temperatures will require significantly reduced assay time to minimize the effect of sample evaporation on the measurement of k_a, k_d or K_D values.

Lack of sensitivity required to characterize picomolar affinity interactions continues to be a challenge for the Octet HTX. Two major problems are associated with the study of picomolar affinity interactions on the Octet biosensor: (i) designing kinetic assays using ultra-low density ligand surface to overcome MTL and (ii) characterization of interactions with slow dissociation rates. Kinetic assays performed on 0.1 nm mAb surface density reduced MTL for all seven picomolar affinity interactions characterized in this study and the binding kinetic parameters measured on Octet HTX correlated with MASS-1 (**Table 3**). However, the measured binding signal was found to be close to the detection limit of the Octet HTX, especially for mAb-1 binding to 14kD antigen. A poor signal to noise ratio was observed and the sensitivity of the Octet HTX was not high enough to discriminate signal from noise (**Figure 6A**). Smoothing of the raw binding signal was required to observe separation in the binding curves for different antigen concentrations (**Supplementary Figure 4**). We also attempted to characterize high affinity mAb to 3.5kD antigen, but the sensitivity of Octet HTX was not high enough to detect the binding signal from the 0.1 nm mAb surface and the specific signal was found to be below the detectable limit of Octet HTX (data not shown). Therefore, an increase in the sensitivity of the current BLI platform is required to characterize such picomolar affinity interactions using low density ligand surfaces as reported in this embodiment.

Characterization of interactions with slow dissociation rates is another major challenge of the Octet HTX. Even without regeneration, we observed some baseline drift following the capture of mAb using the AHC biosensors which interfered with the characterization of slow dissociating interactions (data not shown).

Although stable baseline was achieved by directly immobilizing the mAb on to the AR2G biosensors, sample evaporation observed during the 2-4 hours of dissociation time interfered with reliable measurement of k_d. Even after multiple attempts, we were unable to reliably characterize interactions with k_d values lower than $5x10^{-5}$ $M^{-1}s^{-1}$ (data not shown). Characterizing such interactions using SPR biosensors was comparatively less challenging and reproducible binding kinetic parameters can be measured using the Biacore 4000 biosensors (data not shown).

The **Figure 8** shows that the AHC biosensors can be regenerated and the measured kinetic values were similar to those generated using Biacore 4000 and MASS-1. We detected baseline drift following the regeneration step and reference subtraction of the binding curves was required for the correction of the observed drift. However, we observed large variability in the baseline drift depending on the lot of the AHC sensors used and characterization of interactions with the k_d value less than 10^{-4} s^{-1} was challenging. We found that the baseline drift can be minimized by allowing equilibration of Octet biosensors in HBS-EBT buffer for at least 15 minutes following the regeneration step (data not shown). However, this will result in extending the experiment time and in turn will lead to sample evaporation. We understand that stable baseline is required for designing kinetic assays and any variability in the baseline drift can have a more profound effect on the reliability and reproducibility of measured rate constants. We therefore do not recommend sensor regeneration and use fresh Octet biosensors for the kinetic analysis of biomolecular interactions.

Adopting SCK assay for the characterization of biomolecular interaction is another affordable alternative to the TK assay. Instead of using six to eight Octet biosensors to generate kinetic data using TK assay, concentration dependent antigen binding can be performed using just two Octet biosensors in the SCK assay – one biosensor for reference subtraction and another for antigen binding. The data presented in this work provide enough evidence on the reliability and reproducibility of the SCK assay on Octet HTX (**Figure 3**, **Figure 4**, **Figure 5**, **Supplementary Figure 3** and **Table 2**). However, the users will require a third party analysis software, such as BIAevaluation (version 4.1.1) or CLAMP to fit the data, which can be considered as the limitation of performing SCK assay on the Octet platform. The primary focus of this study was to identify appropriate experimental conditions to characterize mAb-antigen interactions and although investigating the application of the Octet biosensors to study receptor-ligand interactions is beyond the scope of this study, lack of these data can be considered as a limitation of the manuscript.

In this study, numerous kinetic assays were performed by capturing human mAbs on to the AHC Octet biosensors. A total of 165 kinetically diverse human mAbs characterized in this study is our attempt to provide appropriate experimental conditions required to characterize antibody-antigen interactions using the AHC Octet biosensors. However, in order to establish a generic guideline to design kinetic assay on the Octet platform, additional studies will be required using different currently available Octet biosensors – anti-mouse Fc (AMC), anti-human Fab (FAB2G), and amine reactive (AR2G) that are recommended to perform kinetic assay on the Octet platform. Although further optimization of experimental conditions will be required for designing kinetic assays using other Octet biosensors, various experimental conditions and assay optimization considerations presented in this embodiment can be used as guidelines for designing such assays.

In summary, the results presented in this work provide insight on various considerations required to reliably measure k_a, k_d and K_D values of antibody-antigen interactions on the Octet platform along with the limitations involved during the design of kinetic assay. We believe that these data will assist the entire label-free user community to design mAb-antigen kinetic assays on the Octet biosensors. The various experimental conditions and external factors considered in this embodiment to generate reliable and reproducible Octet data will aid the label-free users to make educated decision before selecting appropriate biosensor for their binding studies.

ACKNOWLEDGEMENT:

The authors would like to thank Joel Martin and his group for cloning and purification of all the reagents used in this study. The authors are also thankful to Katrina Fracchiolla, Tammy Huang, and William Olson for critically reading the manuscript and providing their valuable input.

Disclosure Summary:

All the authors are employees and shareholders of Regeneron Pharmaceuticals.

References:

1. Leonard, P., Safsten, P., Hearty, S., McDonnell, B., Finlay, W., and O'Kennedy, R. (2007) High throughput ranking of recombinant avian scFv antibody fragments from crude lysates using the Biacore A100. *J Immunol Methods* **323**, 172-179
2. Katayama, M., Sato, T., and Kuromitsu, J. (2012) Capture molecules preconditioned for kinetic analysis of high-affinity antigen-antibody complex in Biacore A100. *Anal Biochem* **424**, 168-177
3. Abdiche, Y. N., Miles, A., Eckman, J., Foletti, D., Van Blarcom, T. J., Yeung, Y. A., Pons, J., and Rajpal, A. (2014) High-throughput epitope binning assays on label-free array-based biosensors can yield exquisite epitope discrimination that facilitates the selection of monoclonal antibodies with functional activity. *PLoS One* **9**, e92451
4. Leonard, P., Hayes, C. J., and O'Kennedy, R. (2011) Rapid temperature-dependent antibody ranking using Biacore A100. *Anal Biochem* **409**, 290-292
5. Nahshol, O., Bronner, V., Notcovich, A., Rubrecht, L., Laune, D., and Bravman, T. (2008) Parallel kinetic analysis and affinity determination of hundreds of monoclonal antibodies using the ProteOn XPR36. *Anal Biochem* **383**, 52-60
6. Kamat, V., and Rafique, A. (2017) Exploring sensitivity and throughput of a parallel flow SPRi biosensor for characterization of antibody-antigen interaction. *Analytical Biochemistry* **525**, 8-22
7. Keighley, W. (2011) The need for high throughput kinetics early in the drug discovery process. *Drug Discovery World* **12**, 7
8. Lad, L., Clancy, S., Kovalenko, M., Liu, C., Hui, T., Smith, V., and Pagratis, N. (2015) High-throughput kinetic screening of hybridomas to identify high-affinity antibodies using bio-layer interferometry. *J Biomol Screen* **20**, 498-507
9. Yu, Y., Mitchell, S., Lynaugh, H., Brown, M., Nobrega, R. P., Zhi, X., Sun, T., Caffry, I., Cao, Y., Yang, R., Burnina, I., Xu, Y., and Estep, P. (2016) Understanding ForteBio's Sensors for High-Throughput Kinetic and Epitope Screening for Purified Antibodies and Yeast Culture Supernatant. *J Biomol Screen* **21**, 88-95
10. Do, T., Ho, F., Heidecker, B., Witte, K., Chang, L., and Lerner, L. (2008) A rapid method for determining dynamic binding capacity of resins for the purification of proteins. *Protein Expr Purif* **60**, 147-150
11. de Kruif, J., Kramer, A., Nijhuis, R., van der Zande, V., den Blanken, R., Clements, C., Visser, T., Keehnen, R., den Hartog, M., Throsby, M., and Logtenberg, T. (2010) Generation of stable cell clones expressing mixtures of human antibodies. *Biotechnol Bioeng* **106**, 741-750
12. Concepcion, J., Witte, K., Wartchow, C., Choo, S., Yao, D., Persson, H., Wei, J., Li, P., Heidecker, B., Ma, W., Varma, R., Zhao, L. S., Perillat, D., Carricato, G., Recknor, M., Du, K., Ho, H., Ellis, T., Gamez, J., Howes, M., Phi-Wilson, J., Lockard, S., Zuk, R., and Tan, H. (2009) Label-free detection

of biomolecular interactions using BioLayer interferometry for kinetic characterization. *Comb Chem High Throughput Screen* **12**, 791-800

13. Dysinger, M., and King, L. E. (2012) Practical quantitative and kinetic applications of bio-layer interferometry for toxicokinetic analysis of a monoclonal antibody therapeutic. *J Immunol Methods* **379**, 30-41
14. Abdiche, Y. N., Malashock, D. S., Pinkerton, A., and Pons, J. (2009) Exploring blocking assays using Octet, ProteOn, and Biacore biosensors. *Anal Biochem* **386**, 172-180
15. Carney, P. J., Lipatov, A. S., Monto, A. S., Donis, R. O., and Stevens, J. (2010) Flexible label-free quantitative assay for antibodies to influenza virus hemagglutinins. *Clin Vaccine Immunol* **17**, 1407-1416
16. Li, J., Schantz, A., Schwegler, M., and Shankar, G. (2011) Detection of low-affinity anti-drug antibodies and improved drug tolerance in immunogenicity testing by Octet((R)) biolayer interferometry. *J Pharm Biomed Anal* **54**, 286-294
17. Ylera, F., Harth, S., Waldherr, D., Frisch, C., and Knappik, A. (2013) Off-rate screening for selection of high-affinity anti-drug antibodies. *Anal Biochem* **441**, 208-213
18. Barnard, G. C., Kull, A. R., Sharkey, N. S., Shaikh, S. S., Rittenhour, A. M., Burnina, I., Jiang, Y., Li, F., Lynaugh, H., Mitchell, T., Nett, J. H., Nylen, A., Potgieter, T. I., Prinz, B., Rios, S. E., Zha, D., Sethuraman, N., Stadheim, T. A., and Bobrowicz, P. (2010) High-throughput screening and selection of yeast cell lines expressing monoclonal antibodies. *J Ind Microbiol Biotechnol* **37**, 961-971
19. Abdiche, Y., Malashock, D., Pinkerton, A., and Pons, J. (2008) Determining kinetics and affinities of protein interactions using a parallel real-time label-free biosensor, the Octet. *Anal Biochem* **377**, 209-217
20. Yang, D., Singh, A., Wu, H., and Kroe-Barrett, R. (2016) Comparison of biosensor platforms in the evaluation of high affinity antibody-antigen binding kinetics. *Anal Biochem* **508**, 78-96
21. Karlsson, R., Katsamba, P. S., Nordin, H., Pol, E., and Myszka, D. G. (2006) Analyzing a kinetic titration series using affinity biosensors. *Anal Biochem* **349**, 136-147
22. Rich, R. L., Cannon, M. J., Jenkins, J., Pandian, P., Sundaram, S., Magyar, R., Brockman, J., Lambert, J., and Myszka, D. G. (2008) Extracting kinetic rate constants from surface plasmon resonance array systems. *Anal Biochem* **373**, 112-120
23. Bravman, T., Bronner, V., Lavie, K., Notcovich, A., Papalia, G. A., and Myszka, D. G. (2006) Exploring "one-shot" kinetics and small molecule analysis using the ProteOn XPR36 array biosensor. *Anal Biochem* **358**, 281-288
24. Kumaraswamy, S., and Tobias, R. (2015) Label-Free Kinetic Analysis of an Antibody–Antigen Interaction Using Biolayer Interferometry. in *Protein-Protein Interactions: Methods and Applications* (Meyerkord, L. C., and Fu, H. eds.), Springer New York, New York, NY. pp 165-182
25. Frenzel, D., and Willbold, D. (2014) Kinetic titration series with biolayer interferometry. *PLoS One* **9**, e106882
26. Kamat, V., and Rafique, A. Extending the throughput of Biacore 4000 biosensor to accelerate kinetic analysis of antibody-antigen interaction. *Analytical Biochemistry*
27. Myszka, D. G. (1999) Improving biosensor analysis. *J Mol Recognit* **12**, 279-284
28. Abdiche, Y. N., Lindquist, K. C., Pinkerton, A., Pons, J., and Rajpal, A. (2011) Expanding the ProteOn XPR36 biosensor into a 36-ligand array expedites protein interaction analysis. *Anal Biochem* **411**, 139-151
29. Myszka, D. G., He, X., Dembo, M., Morton, T. A., and Goldstein, B. (1998) Extending the range of rate constants available from BIACORE: interpreting mass transport-influenced binding data. *Biophys J* **75**, 583-594

30. Myszka, D. G., Arulanantham, P. R., Sana, T., Wu, Z., Morton, T. A., and Ciardelli, T. L. (1996) Kinetic analysis of ligand binding to interleukin-2 receptor complexes created on an optical biosensor surface. *Protein Sci* **5**, 2468-2478

Supplementary Figures:

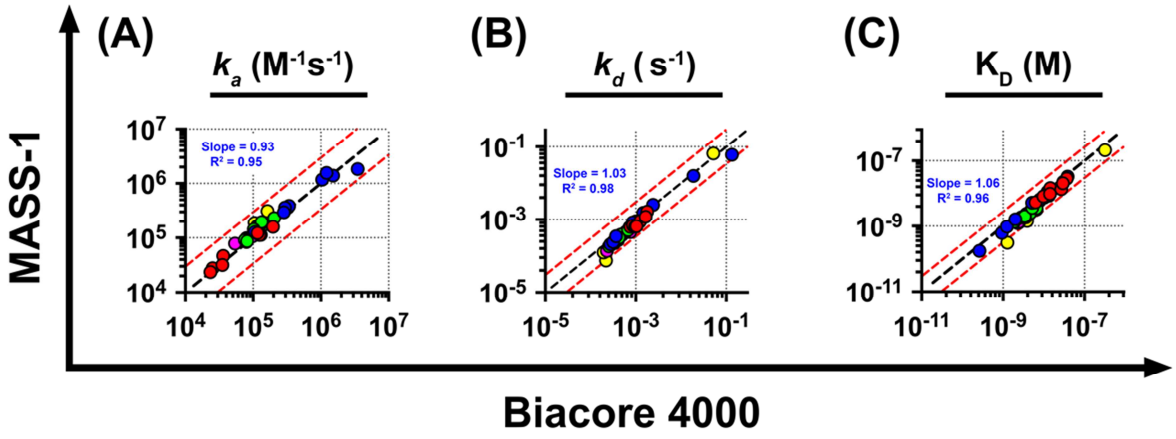

Supplementary Figure 1: Correlation of the binding kinetic parameters measured using MASS-1 & Biacore 4000

Graphical representation showing the correlation of binding kinetic values measured for mAb binding to 20kD (red), 28kD (blue), 39kD (green), 48kD (magenta), and 68kD (yellow) antigen. The values of k_a (**A**), k_d (**B**) and K_D (**C**) measured using Biacore 4000 and MASS-1 are plotted on the x-axis and y-axis, respectively. The scatter plots were fit using a linear regression fit and the slope of the trend line (black serrated line) along with the correlation coefficients (R^2) is shown in the plot. The two serrated red lines represent three-fold difference in the measured values.

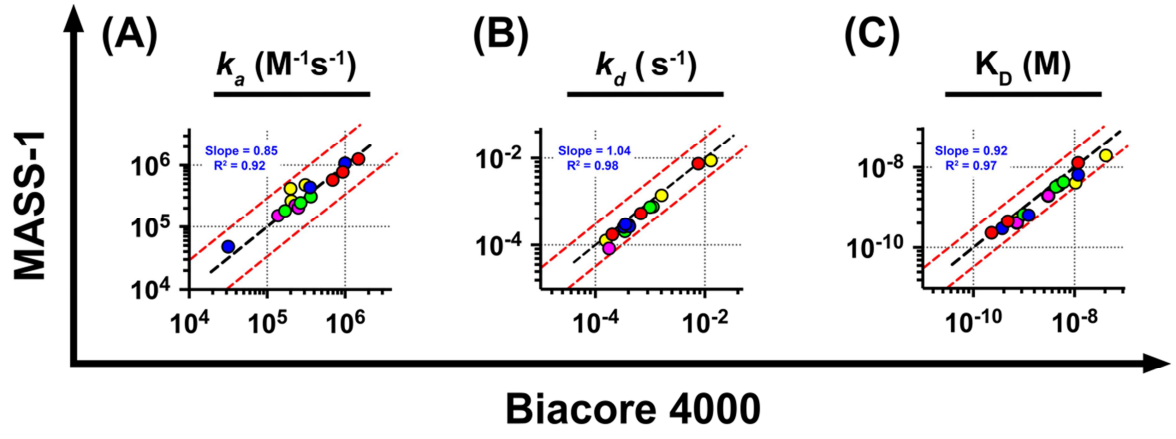

Supplementary Figure 2: Correlation of the binding kinetic parameters measured using MASS-1 and Biacore 4000

Graphical representation showing the correlation of average binding kinetic values measured from at least three independent experiments for mAb binding to 14kD (●), 29kD (●), 48kD (●), 68kD (●), or 105kD (●) antigen. The values of k_a (**A**), k_d (**B**) and

K_D (**C**) measured using Biacore 4000 and MASS-1 are plotted on the x-axis and y-axis, respectively. The scatter plots were fit using a linear regression fit and the slope of the trend line (black serrated line) along with the correlation coefficients (R^2) is shown in the plot. The two serrated red lines represent three-fold difference in the measured values.

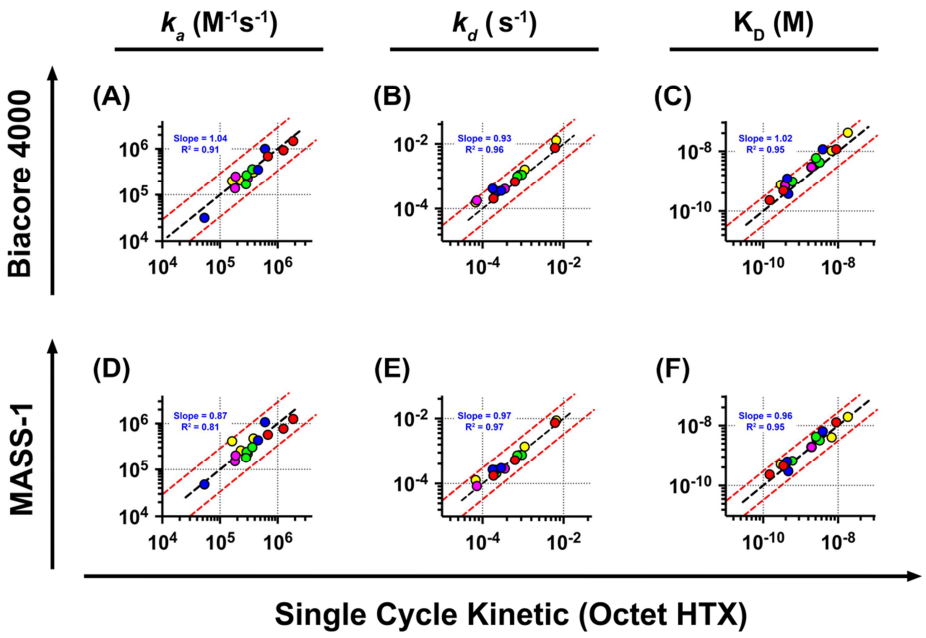

Supplementary Figure 3: Correlation of the binding kinetic values generated using single cycle kinetic assay on Octet HTX with those measured using titration kinetic assay on MASS-1 and Biacore 4000

Graphical representation showing the correlation of average values of k_a (**A**), k_d (**B**) and K_D (**C**) measured from at least three independent experiments for mAbs binding to 14kD (●), 29kD (●), 48kD (●), 68kD (●), or 105kD (●) antigen. The kinetic values calculated using single cycle kinetic assay on Octet HTX is plotted on the x-axis while those measured using titration kinetic assay on Biacore 4000 or MASS-1 is plotted on the y-axis. The scatter plots were fit using a linear regression fit and the slope of the trend line (black serrated line) along with the correlation coefficients (R^2) is shown in the plot. The two serrated red lines represent three-fold difference in the measured values.

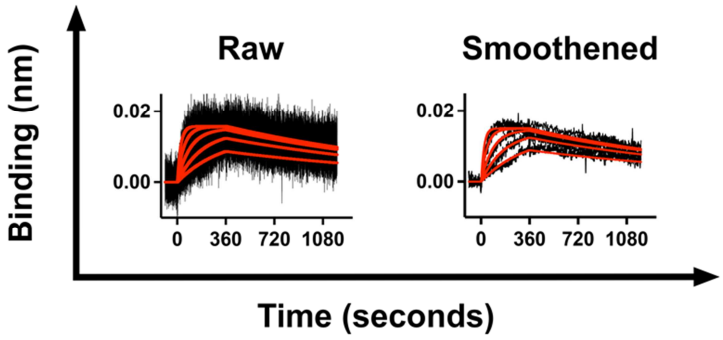

Supplementary Figure 4: Smoothening of Octet binding data

The raw binding data generated for mAb-1 binding to 14kD antigen was smoothened in GraphPad Prism software using the fourth order smoothing with averaging of 20 neighboring data points. The fit generated using the raw binding response was later superimposed on top of the smoothened curve.

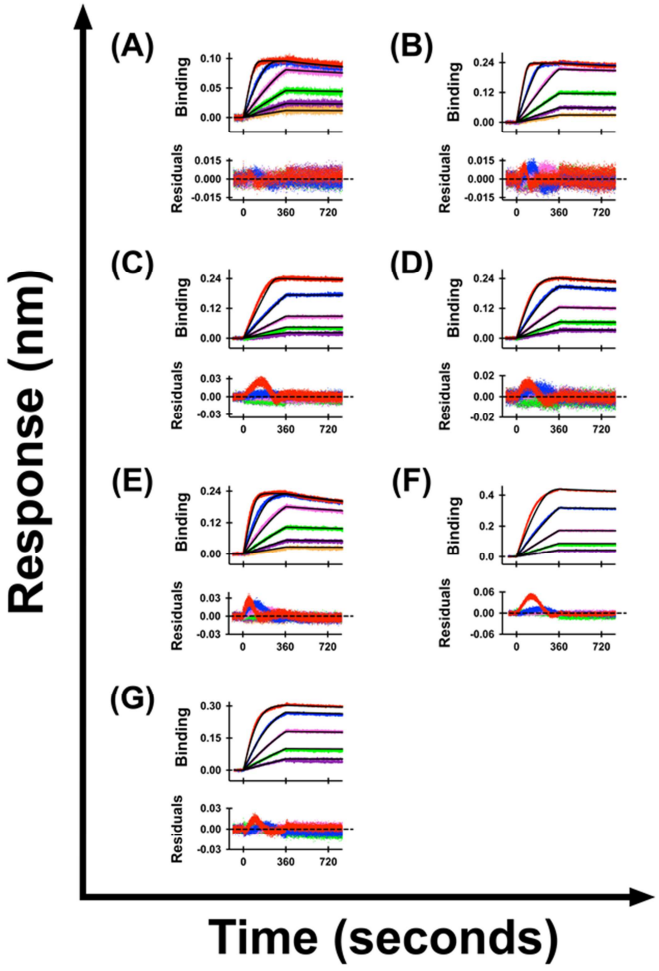

Supplementary Figure 5: Fits of the binding sensorgrams along with the respective residuals observed during the characterization of picomolar affinity mAbs characterized using 0.5nm density surface

Around 0.5nm density mAb binding to binding to 14kD (**A**), 39kD (**B**, **C**, **D**, **E**) or 71kD (**F, G**) antigen was captured using AHC Octet sensors and different concentrations of antigen were allowed to bind for 6 minutes followed by a 15 minute dissociation phase. Real time binding of antigen at varying concentrations is highlighted in different colors while the global fits generated by fitting the data using 1:1 Langmuir binding model with mass transport limitation is shown in serrated black lines. The residuals showing the difference between the experimental data and fits generated is also shown. Non-randomly distributed residuals were observed, especially during the association phase of mAb-3 (**C**), mAb-4 (**D**), mAb-5 (**E**), mAb-6 (**F**), and mAb-7 (**G**) and were found to be greater than 5% of observed binding response.

Supplementary Table 1: Binding kinetics values of 40 mAb-antigen interactions characterized using single capture density on Biacore 4000, MASS-1 and varying capture densities on Octet HTX.

		Biacore 4000			MASS-1			Octet HTX															
	mAb Captured	k_a (1/Ms)	k_d (1/s)	K_D (M)	k_a (1/Ms)	k_d (1/s)	K_D (M)	mAb Capture Level (nm)	k_a (1/Ms)	k_d (1/s)	K_D (M)	mAb Capture Level (nm)	k_a (1/Ms)	k_d (1/s)	K_D (M)	mAb Capture Level (nm)	k_a (1/Ms)	k_d (1/s)	K_D (M)	mAb Capture Level (nm)	k_a (1/Ms)	k_d (1/s)	K_D (M)
Antigen-1 (20kD)	mAb-1	2.52E+04	7.57E-04	3.00E-08	2.77E+04	6.23E-04	2.25E-08	0.17	2.73E+04	5.55E-04	2.04E-08	0.32	3.10E+04	6.58E-04	2.12E-08	0.54	3.08E+04	6.33E-04	2.05E-08	0.95	3.02E+04	7.37E-04	2.44E-08
	mAb-2	1.96E+05	1.23E-03	6.25E-09	1.59E+05	8.53E-04	5.38E-09	0.22	1.75E+05	4.75E-04	2.72E-09	0.42	1.82E+05	5.75E-04	3.17E-09	0.70	1.76E+05	6.73E-04	3.82E-09	1.22	1.46E+05	7.27E-04	4.97E-09
	mAb-3	1.30E+05	1.27E-03	9.77E-09	1.13E+05	9.18E-04	8.12E-09	0.18	8.71E+04	4.49E-04	5.16E-09	0.33	8.64E+04	7.16E-04	8.29E-09	0.56	8.72E+04	8.04E-04	9.21E-09	1.00	7.10E+04	1.01E-03	1.41E-08
	mAb-4	1.24E+05	1.78E-03	1.44E-08	1.12E+05	1.64E-03	1.46E-08	0.21	1.17E+05	9.68E-04	8.27E-09	0.37	1.15E+05	1.62E-03	1.41E-08	0.61	1.08E+05	1.33E-03	1.23E-08	0.98	9.71E+04	1.25E-03	1.29E-08
	mAb-5	2.34E+04	8.60E-04	3.67E-08	2.36E+04	6.75E-04	2.86E-08	0.19	3.83E+04	7.67E-04	2.00E-08	0.35	3.50E+04	8.12E-04	2.32E-08	0.57	3.09E+04	7.10E-04	2.29E-08	0.99	3.19E+04	7.22E-04	2.26E-08
	mAb-6	1.16E+05	1.65E-03	1.42E-08	1.22E+05	1.18E-03	9.72E-09	0.21	1.54E+05	1.35E-03	8.77E-09	0.40	1.57E+05	1.26E-03	8.02E-09	0.66	1.48E+05	1.20E-03	8.13E-09	1.11	1.35E+05	1.11E-03	8.18E-09
	mAb-7	3.62E+04	9.69E-04	2.68E-08	4.65E+04	6.31E-04	1.36E-08	0.23	5.17E+04	3.97E-04	7.68E-09	0.41	5.00E+04	5.03E-04	1.01E-08	0.66	4.78E+04	4.92E-04	1.03E-08	1.07	4.64E+04	5.24E-04	1.13E-08
	mAb-8	3.52E+04	1.03E-03	2.93E-08	3.17E+04	6.50E-04	2.05E-08	0.25	5.20E+04	2.58E-04	4.97E-09	0.46	5.24E+04	4.25E-04	8.11E-09	0.77	5.45E+04	5.22E-04	9.58E-09	1.25	5.11E+04	5.21E-04	1.02E-08
Antigen-2 (28kD)	mAb-1	1.04E+06	2.73E-04	2.62E-10	1.18E+06	2.07E-04	1.76E-10	0.20	1.03E+06	1.60E-04	1.55E-10	0.37	6.28E+05	1.97E-04	3.14E-10	0.60	7.73E+05	1.81E-04	2.34E-10	1.00	3.21E+05	1.38E-04	4.30E-10
	mAb-2	1.51E+06	1.88E-02	1.24E-08	1.39E+06	1.58E-02	1.13E-08	0.22	1.78E+06	1.21E-02	6.77E-09	0.43	8.84E+05	9.35E-03	1.06E-08	0.68	7.71E+05	9.52E-03	1.23E-08	1.12	5.25E+05	8.65E-03	1.65E-08
	mAb-3	3.38E+05	3.15E-04	9.31E-10	3.86E+05	2.39E-04	6.20E-10	0.19	4.44E+05	3.10E-04	6.98E-10	0.38	3.47E+05	3.52E-04	1.02E-09	0.62	3.39E+05	2.53E-04	7.48E-10	1.08	2.72E+05	2.53E-04	9.28E-10
	mAb-4	1.06E+05	8.54E-04	8.05E-09	1.28E+05	8.36E-04	6.55E-09	0.13	1.27E+05	2.23E-04	1.76E-09	0.37	1.61E+05	7.20E-04	4.47E-09	0.61	1.47E+05	7.49E-04	5.09E-09	1.05	1.22E+05	6.52E-04	5.33E-09
	mAb-5	2.95E+05	3.65E-04	1.24E-09	3.59E+05	3.45E-04	9.63E-10	0.19	4.69E+05	6.14E-04	1.31E-09	0.38	3.17E+05	3.66E-04	1.15E-09	0.63	3.11E+05	4.11E-04	1.32E-09	1.12	2.54E+05	3.00E-04	1.18E-09
	mAb-6	3.49E+06	1.34E-01	3.83E-08	1.83E+06	6.01E-02	3.28E-08	0.22	4.00E+06	1.05E-01	2.64E-08	0.41	2.21E+06	5.62E-02	2.54E-08	0.70	1.47E+06	4.69E-02	3.18E-08	1.22	6.01E+05	2.78E-02	4.63E-08
	mAb-7	1.21E+06	2.41E-03	1.99E-09	1.56E+06	2.54E-03	1.62E-09	0.23	1.16E+06	2.08E-03	1.79E-09	0.45	8.34E+05	1.67E-03	2.00E-09	0.73	5.38E+05	1.32E-03	2.45E-09	1.19	3.29E+05	1.22E-03	3.70E-09
	mAb-8	2.84E+05	1.46E-03	5.15E-09	2.95E+05	1.53E-03	5.20E-09	0.26	3.46E+05	1.22E-03	3.53E-09	0.48	2.69E+05	1.30E-03	4.81E-09	0.80	2.74E+05	1.08E-03	3.93E-09	1.28	2.30E+05	9.94E-04	4.33E-09
Antigen-3 (39kD)	mAb-1	1.27E+05	1.69E-03	1.33E-08	1.81E+05	1.55E-03	8.59E-09	0.20	1.66E+05	9.42E-04	5.67E-09	0.38	1.97E+05	1.56E-03	7.93E-09	0.66	1.65E+05	1.37E-03	8.29E-09	1.01	1.48E+05	1.39E-03	9.40E-09
	mAb-2	1.32E+05	7.27E-04	5.52E-09	1.56E+05	6.05E-04	3.88E-09	0.18	1.50E+05	6.34E-04	4.23E-09	0.34	1.24E+05	6.79E-04	5.47E-09	0.55	1.03E+05	5.71E-04	5.54E-09	0.91	8.64E+04	5.49E-04	6.35E-09
	mAb-3	1.29E+05	5.95E-04	4.60E-09	1.78E+05	4.45E-04	2.50E-09	0.18	1.98E+05	5.06E-04	2.55E-09	0.35	1.79E+05	4.79E-04	2.67E-09	0.61	1.58E+05	4.30E-04	2.72E-09	1.01	1.41E+05	4.05E-04	2.88E-09
	mAb-4	1.34E+05	4.64E-04	3.47E-09	1.96E+05	3.80E-04	1.94E-09	0.22	2.03E+05	2.77E-04	1.37E-09	0.40	1.77E+05	3.09E-04	1.74E-09	0.69	1.57E+05	3.45E-04	2.19E-09	1.10	1.39E+05	3.30E-04	2.38E-09
	mAb-5	1.02E+05	6.77E-04	6.63E-09	1.42E+05	5.08E-04	3.57E-09	0.21	1.84E+05	7.44E-04	4.05E-09	0.40	1.58E+05	5.38E-04	3.41E-09	0.69	1.45E+05	4.57E-04	3.15E-09	1.09	1.28E+05	4.70E-04	3.67E-09
	mAb-6	7.55E+04	2.56E-04	3.39E-09	9.10E+04	1.82E-04	2.00E-09	0.17	1.12E+05	1.71E-04	1.53E-09	0.31	1.02E+05	1.96E-04	1.93E-09	0.53	9.75E+04	1.72E-04	1.77E-09	0.85	8.76E+04	1.72E-04	1.97E-09
	mAb-7	2.04E+05	3.90E-04	1.91E-09	2.31E+05	3.15E-04	1.36E-09	0.21	1.95E+05	1.80E-04	9.21E-10	0.38	1.69E+05	2.44E-04	1.45E-09	0.66	1.48E+05	3.00E-04	2.03E-09	1.05	1.27E+05	2.46E-04	1.94E-09
	mAb-8	8.13E+04	4.22E-04	5.19E-09	8.62E+04	3.15E-04	3.66E-09	0.21	9.66E+04	2.75E-04	2.85E-09	0.38	9.15E+04	2.73E-04	2.98E-09	0.67	9.02E+04	3.24E-04	3.60E-09	1.06	8.57E+04	2.99E-04	3.49E-09
Antigen-4 (48kD)	mAb-1	8.46E+04	3.11E-04	3.68E-09	9.60E+04	2.18E-04	2.27E-09	0.21	1.34E+05	1.24E-04	9.26E-10	0.38	1.26E+05	1.75E-04	1.38E-09	0.68	1.16E+05	1.70E-04	1.46E-09	1.17	1.04E+05	2.00E-04	1.93E-09
	mAb-2	1.14E+05	4.09E-04	3.58E-09	1.62E+05	3.04E-04	1.88E-09	0.24	2.00E+05	2.63E-04	1.32E-09	0.42	1.90E+05	2.32E-04	1.22E-09	0.68	1.73E+05	2.53E-04	1.46E-09	1.09	1.57E+05	2.64E-04	1.68E-09
	mAb-3	7.97E+04	4.06E-04	5.09E-09	8.38E+04	2.78E-04	3.32E-09	0.23	1.57E+05	1.96E-04	1.25E-09	0.40	1.55E+05	2.73E-04	1.76E-09	0.64	1.39E+05	2.25E-04	1.62E-09	1.03	1.31E+05	2.44E-04	1.86E-09
	mAb-4	1.27E+05	7.48E-04	5.90E-09	1.28E+05	4.46E-04	3.49E-09	0.22	2.21E+05	5.73E-04	2.59E-09	0.36	2.05E+05	6.53E-04	3.19E-09	0.61	1.94E+05	6.85E-04	3.53E-09	1.03	1.72E+05	7.37E-04	4.29E-09
	mAb-5	9.38E+04	2.29E-04	2.44E-09	1.05E+05	1.37E-04	1.31E-09	0.24	1.47E+05	1.49E-04	1.02E-09	0.42	1.38E+05	1.35E-04	9.84E-10	0.66	1.28E+05	1.05E-04	8.19E-10	1.06	1.20E+05	1.27E-04	1.05E-09
	mAb-6	8.69E+04	8.77E-04	1.01E-08	9.79E+04	7.51E-04	7.67E-09	0.24	1.28E+05	6.52E-04	5.09E-09	0.40	1.26E+05	6.88E-04	5.47E-09	0.63	1.22E+05	6.37E-04	5.24E-09	1.01	1.11E+05	6.10E-04	5.50E-09
	mAb-7	5.40E+04	3.54E-04	6.55E-09	7.82E+04	2.59E-04	3.31E-09	0.26	1.05E+05	2.89E-04	2.76E-09	0.43	1.06E+05	1.82E-04	1.72E-09	0.67	9.99E+04	2.30E-04	2.31E-09	1.06	9.38E+04	2.35E-04	2.51E-09
	mAb-8	9.76E+04	2.74E-04	2.80E-09	1.06E+05	1.95E-04	1.84E-09	0.24	1.33E+05	2.17E-04	1.63E-09	0.42	1.31E+05	1.37E-04	1.04E-09	0.69	1.23E+05	1.49E-04	1.21E-09	1.14	1.17E+05	1.69E-04	1.44E-09
Antigen-5 (68kD)	mAb-1	1.48E+05	3.34E-04	2.26E-09	1.80E+05	2.22E-04	1.23E-09	0.22	2.92E+05	1.65E-04	5.66E-10	0.40	2.66E+05	3.36E-04	1.26E-09	0.65	2.45E+05	2.86E-04	1.17E-09	1.08	2.14E+05	2.68E-04	1.25E-09
	mAb-2	1.73E+05	2.19E-04	1.27E-09	2.39E+05	7.45E-05	3.12E-10	0.21	3.27E+05	9.05E-05	2.79E-10	0.37	2.97E+05	1.32E-04	4.44E-10	0.62	2.57E+05	8.04E-05	3.11E-10	1.04	2.24E+05	1.16E-04	5.18E-10
	mAb-3	7.96E+04	1.94E-04	2.44E-09	9.81E+04	1.24E-04	1.26E-09	0.22	1.54E+05	1.26E-04	8.17E-10	0.40	1.52E+05	1.25E-04	8.22E-10	0.65	1.42E+05	1.13E-04	7.95E-10	1.07	1.35E+05	1.14E-04	8.46E-10
	mAb-4	1.05E+05	4.06E-04	3.86E-09	1.88E+05	2.69E-04	1.43E-09	0.27	2.13E+05	2.28E-04	1.07E-09	0.45	1.97E+05	2.81E-04	1.43E-09	0.71	1.79E+05	2.87E-04	1.61E-09	1.11	1.64E+05	3.07E-04	1.87E-09
	mAb-5	1.31E+05	4.95E-04	3.78E-09	1.56E+05	3.73E-04	2.40E-09	0.25	1.84E+05	4.93E-04	2.67E-09	0.44	1.72E+05	5.08E-04	2.96E-09	0.70	1.54E+05	4.49E-04	2.92E-09	1.12	1.45E+05	4.61E-04	3.19E-09
	mAb-6	1.28E+05	1.00E-03	7.82E-09	1.52E+05	9.01E-04	5.93E-09	0.26	1.90E+05	6.82E-04	3.59E-09	0.46	1.75E+05	6.57E-04	3.76E-09	0.74	1.62E+05	6.66E-04	4.11E-09	1.15	1.52E+05	6.37E-04	4.18E-09
	mAb-7	3.25E+05	6.58E-04	2.03E-09	3.60E+05	4.95E-04	1.37E-09	0.19	4.62E+05	7.85E-04	1.70E-09	0.35	4.01E+05	6.12E-04	1.53E-09	0.61	3.34E+05	6.07E-04	1.82E-09	1.10	2.64E+05	5.51E-04	2.09E-09
	mAb-8	1.63E+05	5.17E-02	3.18E-07	3.12E+05	6.52E-02	2.09E-07	0.21	2.29E+05	4.54E-02	1.99E-07	0.39	2.44E+05	4.29E-02	1.76E-07	0.63	2.52E+05	4.59E-02	1.82E-07	1.02	3.23E+05	5.19E-02	1.61E-07

The results of the kinetic analysis performed to identify appropriate capture density for reliable measurement of binding kinetic values on the Octet HTX are provided in the table. A total of 40 mAbs to antigens with molecular weights of 20kD, 28kD, 39kD, 48kD, and 68kD (eight mAbs per antigen) were first characterized on Biacore 4000 and MASS-1. Based on these results, the highest antigen concentration used to fit the real time binding curves generated on Biacore 4000 or MASS-1was selected and all the 40 mAb-antigen interactions were later studied at varying capture densities (as indicated in the table) on Octet HTX.

Table 1

Antigen Molecular Weight	mAb Captured	Biacore 4000			MASS-1			Octet HTX											
		k_a (1/Ms)	k_d (1/s)	K_D (M)	k_a (1/Ms)	k_d (1/s)	K_D (M)	Capture Level (nm)	k_a (1/Ms)	k_d (1/s)	K_D (M)	Capture Level (nm)	k_a (1/Ms)	k_d (1/s)	K_D (M)	Capture Level (nm)	k_a (1/Ms)	k_d (1/s)	K_D (M)
20kD	mAb-1	2.52×10^{4}	7.57×10^{-4}	3.00×10^{-8}	2.77×10^{4}	6.23×10^{-4}	2.25×10^{-8}	0.17	2.73×10^{4}	5.55×10^{-4}	2.04×10^{-8}	0.32	3.10×10^{4}	6.58×10^{-4}	2.12×10^{-8}	0.54	3.08×10^{4}	6.33×10^{-4}	2.05×10^{-8}	0.95	3.02×10^{4}	7.37×10^{-4}	2.44×10^{-8}
	mAb-2	1.96×10^{5}	1.23×10^{-3}	6.25×10^{-9}	1.59×10^{5}	8.53×10^{-4}	5.38×10^{-9}	0.22	1.75×10^{5}	4.75×10^{-4}	2.72×10^{-9}	0.42	1.82×10^{5}	5.75×10^{-4}	3.17×10^{-9}	0.70	1.76×10^{5}	6.73×10^{-4}	3.82×10^{-9}	1.22	1.46×10^{5}	7.27×10^{-4}	4.97×10^{-9}
28kD	mAb-1	1.04×10^{6}	2.73×10^{-4}	2.62×10^{-10}	1.18×10^{6}	2.07×10^{-4}	1.76×10^{-10}	0.20	1.03×10^{6}	1.60×10^{-4}	1.55×10^{-10}	0.37	6.28×10^{5}	1.97×10^{-4}	3.14×10^{-10}	0.60	7.73×10^{5}	1.81×10^{-4}	2.34×10^{-10}	1.00	3.21×10^{5}	1.38×10^{-4}	4.30×10^{-10}
	mAb-2	1.51×10^{6}	1.88×10^{-2}	1.24×10^{-8}	1.39×10^{6}	1.58×10^{-2}	1.13×10^{-8}	0.22	1.78×10^{6}	1.21×10^{-2}	6.77×10^{-9}	0.43	8.84×10^{5}	9.35×10^{-3}	1.06×10^{-9}	0.68	7.71×10^{5}	9.52×10^{-3}	1.23×10^{-8}	1.12	5.25×10^{5}	8.65×10^{-3}	1.65×10^{-8}
39kD	mAb-1	1.27×10^{5}	1.69×10^{-3}	1.33×10^{-8}	1.81×10^{5}	1.55×10^{-3}	8.59×10^{-9}	0.20	1.66×10^{5}	9.42×10^{-4}	5.67×10^{-9}	0.38	1.97×10^{5}	1.56×10^{-3}	7.93×10^{-9}	0.66	1.65×10^{5}	1.37×10^{-3}	8.29×10^{-9}	1.01	1.48×10^{5}	1.39×10^{-3}	9.40×10^{-9}
	mAb-2	1.32×10^{5}	7.27×10^{-4}	5.52×10^{-9}	1.56×10^{5}	6.05×10^{-4}	3.88×10^{-9}	0.18	1.50×10^{5}	6.34×10^{-4}	4.23×10^{-9}	0.34	1.24×10^{5}	6.79×10^{-4}	5.47×10^{-9}	0.55	1.03×10^{5}	5.71×10^{-4}	5.54×10^{-9}	0.91	8.64×10^{4}	5.49×10^{-4}	6.35×10^{-9}
48kD	mAb-1	8.46×10^{4}	3.11×10^{-4}	3.68×10^{-9}	9.60×10^{4}	2.18×10^{-4}	2.27×10^{-9}	0.21	1.34×10^{5}	1.24×10^{-4}	9.26×10^{-10}	0.38	1.26×10^{5}	1.75×10^{-4}	1.38×10^{-9}	0.68	1.16×10^{5}	1.70×10^{-4}	1.46×10^{-9}	1.17	1.04×10^{5}	2.00×10^{-4}	1.93×10^{-9}
	mAb-2	1.14×10^{5}	4.09×10^{-4}	3.58×10^{-9}	1.62×10^{5}	3.04×10^{-4}	1.88×10^{-9}	0.24	2.00×10^{5}	2.63×10^{-4}	1.32×10^{-9}	0.42	1.90×10^{5}	2.32×10^{-4}	1.22×10^{-9}	0.68	1.73×10^{5}	2.53×10^{-4}	1.46×10^{-9}	1.09	1.57×10^{5}	2.64×10^{-4}	1.68×10^{-9}
68kD	mAb-1	1.48×10^{5}	3.34×10^{-4}	2.26×10^{-9}	1.80×10^{5}	2.22×10^{-4}	1.23×10^{-9}	0.22	2.92×10^{5}	1.65×10^{-4}	5.66×10^{-10}	0.40	2.66×10^{5}	3.36×10^{-4}	1.26×10^{-9}	0.65	2.45×10^{5}	2.86×10^{-4}	1.17×10^{-9}	1.08	2.14×10^{5}	2.68×10^{-4}	1.25×10^{-9}
	mAb-2	1.73×10^{5}	2.19×10^{-4}	1.27×10^{-9}	2.39×10^{5}	7.45×10^{-5}	3.12×10^{-10}	0.21	3.27×10^{5}	9.05×10^{-5}	2.79×10^{-10}	0.37	2.97×10^{5}	1.32×10^{-4}	4.44×10^{-10}	0.62	2.57×10^{5}	8.04×10^{-5}	3.11×10^{-10}	1.04	2.24×10^{5}	1.16×10^{-4}	5.18×10^{-10}

Antigen Molecular Weight	mAb Captured	Biacore 4000			MASS-1			Octet HTX					
		Titration Kinetic (TK)			Titration Kinetic (TK)			Titration Kinetic (TK)			Single Cycle Kinetic		
		k_a ($x10^5$ 1/Ms)	k_d ($x10^{-4}$ 1/s)	K_D ($x10^{-9}$ M)	k_a ($x10^5$ 1/Ms)	k_d ($x10^{-4}$ 1/s)	K_D ($x10^{-9}$ M)	k_a ($x10^5$ 1/Ms)	k_d ($x10^{-4}$ 1/s)	K_D ($x10^{-9}$ M)	k_a ($x10^5$ 1/Ms)	k_d ($x10^{-4}$ 1/s)	K_D ($x10^{-9}$ M)
14kD	**mAb-1**	14.79 ± 2.07	6.82 ± 1.03	0.48 ± 0.16	12.57 ± 3.66	5.27 ± 0.50	0.44 ± 0.12	19.14 ± 2.00	4.69 ± 1.65	0.25 ± 0.11	18.50 ± 0.46	6.36 ± 1.65	0.34 ± 0.08
	mAb-2	6.88 ± 1.16	76.29 ± 13.15	11.67 ± 4.62	5.82 ± 1.12	73.84 ± 10.34	12.84 ± 1.39	6.35 ± 2.11	67.28 ± 2.72	11.65 ± 4.49	6.76 ± 0.62	61.00 ± 13.97	8.96 ± 1.38
	mAb-3	9.29 ± 1.85	2.06 ± 0.14	0.23 ± 0.06	7.77 ± 0.97	1.74 ± 0.14	0.23 ± 0.05	11.54 ± 1.82	2.43 ± 1.14	0.21 ± 0.08	12.47 ± 0.59	1.85 ± 0.66	0.15 ± 0.05
29kD	**mAb-4**	3.55 ± 0.71	4.13 ± 0.57	1.23 ± 0.46	4.40 ± 1.09	2.64 ± 0.35	0.64 ± 0.21	3.58 ± 0.17	2.16 ± 0.47	0.60 ± 0.12	4.58 ± 1.45	1.79 ± 0.35	0.44 ± 0.19
	mAb-5	0.32 ± 0.13	3.31 ± 0.43	11.77 ± 4.86	0.48 ± 0.22	2.58 ± 0.38	6.42 ± 3.42	0.37 ± 0.03	2.06 ± 0.37	5.51 ± 0.57	0.54 ± 0.06	2.11 ± 0.30	3.90 ± 0.47
	mAb-6	9.95 ± 2.05	3.55 ± 0.17	0.37 ± 0.10	10.58 ± 2.71	2.95 ± 0.31	0.30 ± 0.10	5.43 ± 0.89	2.47 ± 0.19	0.46 ± 0.04	6.05 ± 1.15	2.86 ± 0.88	0.47 ± 0.12
48kD	**mAb-7**	3.6 ± 0.18	3.47 ± 0.49	0.97 ± 0.18	3.09 ± 0.54	2.02 ± 0.24	0.66 ± 0.06	3.30 ± 0.22	1.87 ± 0.71	0.56 ± 0.21	3.63 ± 0.41	2.20 ± 0.51	0.60 ± 0.11
	mAb-8	2.67 ± 0.38	11.29 ± 2.55	4.28 ± 1.08	2.46 ± 0.60	7.54 ± 0.18	3.26 ± 1.03	3.04 ± 0.54	6.57 ± 1.08	2.25 ± 0.72	2.86 ± 0.19	9.40 ± 2.83	3.26 ± 0.80
	mAb-9	1.71 ± 0.21	10.05 ± 1.16	5.98 ± 1.30	1.84 ± 0.45	7.45 ± 0.21	4.28 ± 1.29	2.46 ± 0.36	5.98 ± 0.67	2.45 ± 0.35	2.82 ± 0.50	7.21 ± 1.61	2.55 ± 0.25
68kD	**mAb-10**	1.37 ± 0.14	4.1 ± 0.12	3.02 ± 0.29	1.52 ± 0.36	2.81 ± 0.07	1.95 ± 0.55	2.00 ± 0.31	2.33 ± 0.55	1.21 ± 0.43	1.81 ± 0.35	3.59 ± 1.20	1.95 ± 0.39
	mAb-11	2.32 ± 0.27	11.28 ± 1.97	4.92 ± 1.04	2.23 ± 0.50	7.53 ± 0.03	3.54 ± 0.98	2.80 ± 0.16	6.90 ± 0.32	2.46 ± 0.09	2.99 ± 0.36	8.14 ± 2.50	2.71 ± 0.64
	mAb-12	2.52 ± 0.43	1.79 ± 0.12	0.72 ± 0.10	2.02 ± 0.43	0.84 ± 0.23	0.41 ± 0.04	2.10 ± 0.21	0.71 ± 0.02	0.34 ± 0.04	1.86 ± 0.08	0.72 ± 0.10	0.39 ± 0.07
105kD	**mAb-13**	2.05 ± 0.13	1.56 ± 0.39	0.76 ± 0.21	2.62 ± 0.58	1.25 ± 0.62	0.50 ± 0.25	2.58 ± 0.14	0.70 ± 0.01	0.27 ± 0.01	2.28 ± 0.03	0.68 ± 0.08	0.30 ± 0.04
	mAb-14	3.11 ± 0.48	127.86 ± 24.43	41.38 ± 7.74	4.84 ± 1.85	86.45 ± 7.77	19.53 ± 5.98	2.78 ± 0.40	81.00 ± 9.37	29.97 ± 8.34	3.78 ± 0.78	65.60 ± 1.87	18.00 ± 4.78
	mAb-15	2.01 ± 1.04	16.30 ± 1.83	10.40 ± 6.09	4.20 ± 2.37	13.73 ± 1.89	4.07 ± 2.00	1.44 ± 0.27	13.39 ± 1.85	9.76 ± 3.50	1.62 ± 0.13	11.00 ± 0.61	6.81 ± 0.89

Table 3

Antigen Molecular Weight	mAb Captured	MASS-1 Capture Level (RU)	MASS-1 k_m (cm/s)	MASS-1 k_a (1/Ms)	MASS-1 k_d (1/s)	MASS-1 K_D (M)	Octet HTX Capture Level (nm)	Octet HTX k_m (cm/s)	Octet HTX k_a (1/Ms)	Octet HTX k_d (1/s)	Octet HTX K_D (M)
14kD	**mAb-1**	350	8.57×10^{7}	3.29×10^{6}	3.14×10^{-4}	9.54×10^{-11}	0.60	6.39×10^{4}	3.73×10^{6}	2.92×10^{-4}	7.81×10^{-11}
		19	7.54×10^{9}	4.34×10^{6}	2.46×10^{-4}	5.67×10^{-11}	0.12	1.00×10^{10}	4.92×10^{6}	3.30×10^{-4}	6.70×10^{-11}
39kD	**mAb-2**	70	1.51×10^{8}	1.30×10^{7}	1.20×10^{-4}	9.21×10^{-12}	0.50	1.43×10^{5}	7.44×10^{6}	1.24×10^{-4}	1.67×10^{-11}
		6	8.36×10^{9}	1.26×10^{7}	8.06×10^{-5}	6.43×10^{-12}	0.11	9.39×10^{4}	2.05×10^{7}	9.85×10^{-5}	4.81×10^{-12}
	mAb-3	59	1.42×10^{8}	8.10×10^{6}	9.85×10^{-5}	1.22×10^{-11}	0.56	1.98×10^{5}	2.63×10^{6}	1.38×10^{-4}	5.24×10^{-11}
		6	5.00×10^{9}	8.09×10^{6}	4.83×10^{-5}	5.93×10^{-12}	0.11	9.29×10^{4}	8.15×10^{6}	5.47×10^{-5}	6.71×10^{-12}
	mAb-4	60	1.99×10^{8}	4.95×10^{6}	1.50×10^{-4}	3.03×10^{-11}	0.53	1.61×10^{5}	2.42×10^{6}	3.42×10^{-4}	1.41×10^{-10}
		6	1.35×10^{9}	4.76×10^{6}	6.26×10^{-5}	1.32×10^{-11}	0.11	1.44×10^{5}	3.83×10^{6}	9.38×10^{-5}	2.45×10^{-11}
	mAb-5	65	2.63×10^{8}	4.46×10^{6}	3.87×10^{-4}	8.67×10^{-11}	0.53	1.04×10^{5}	1.05×10^{7}	3.85×10^{-5}	3.60×10^{-12}
		6	1.00×10^{10}	5.86×10^{6}	3.52×10^{-4}	6.00×10^{-11}	0.11	5.00×10^{6}	3.41×10^{6}	3.29×10^{-4}	9.64×10^{-11}
71kD	**mAb-6**	32	4.71×10^{8}	6.31×10^{6}	1.50×10^{-4}	2.38×10^{-11}	0.60	2.38×10^{5}	2.80×10^{6}	7.42×10^{-5}	2.65×10^{-11}
		5	1.00×10^{10}	8.21×10^{6}	1.23×10^{-4}	1.50×10^{-11}	0.10	1.00×10^{10}	1.55×10^{7}	1.41×10^{-4}	9.08×10^{-12}
	mAb-7	45	4.44×10^{8}	6.19×10^{6}	7.17×10^{-5}	1.16×10^{-11}	0.40	4.21×10^{5}	1.92×10^{6}	6.10×10^{-5}	3.17×10^{-11}
		6	1.00×10^{10}	7.53×10^{6}	6.88×10^{-5}	9.16×10^{-12}	0.07	1.00×10^{10}	2.81×10^{6}	6.78×10^{-5}	2.41×10^{-11}

Antigen Molecular Weight	mAb Captured	Biacore 4000			MASS-1			Octet HTX		
		k_a ($x10^5$ 1/Ms)	k_d ($x10^{-4}$ 1/s)	K_D ($x10^{-9}$ M)	k_a ($x10^5$ 1/Ms)	k_d ($x10^{-4}$ 1/s)	K_D ($x10^{-9}$ M)	k_a ($x10^5$ 1/Ms)	k_d ($x10^{-4}$ 1/s)	K_D ($x10^{-9}$ M)
21kD	mAb-1	0.33 ± 0.09	35.74 ± 4.27	114.33 ± 38.66	0.39 ± 0.09	25.74 ± 3.91	68.83 ± 21.80	0.33 ± 0.04	53.89 ± 5.52	167.33 ± 41.31
	mAb-2	0.69 ± 0.11	332.47 ± 89.20	478.46 ± 103.81	0.66 ± 0.04	214.33 ± 54.67	321.00 ± 71.51	1.01 ± 0.06	379.57 ± 57.64	378 ± 81.43
	mAb-3	0.42 ± 0.12	39.49 ± 7.83	101.40 ± 40.94	0.44 ± 0.08	30.85 ± 2.36	71.93 ± 16.52	0.58 ± 0.04	50.52 ± 0.50	87.37 ± 5.05
	mAb-4	0.73 ± 0.09	92.83 ± 5.77	127.33 ± 12.66	1.20 ± 0.78	73.48 ± 7.85	76.30 ± 36.63	1.30 ± 0.18	118.43 ± 13.69	91.40 ± 8.27
28kD	mAb-5	4.97 ± 1.70	1.90 ± 0.10	0.41 ± 0.14	3.60 ± 0.22	1.51 ± 0.10	0.42 ± 0.01	2.72 ± 0.30	2.72 ± 0.42	1.00 ± 0.07
	mAb-6	1.82 ± 0.47	3.17 ± 0.13	1.80 ± 0.36	1.20 ± 0.08	3.58 ± 1.01	2.98 ± 0.86	1.78 ± 0.44	5.21 ± 1.55	2.94 ± 0.56
	mAb-7	3.48 ± 0.63	4.24 ± 0.15	1.25 ± 0.24	2.93 ± 0.10	3.82 ± 0.34	1.30 ± 0.07	2.14 ± 0.30	6.15 ± 0.92	2.88 ± 0.27
	mAb-8	5.74 ± 1.81	1.94 ± 0.46	0.38 ± 0.20	3.98 ± 0.40	1.32 ± 0.08	0.33 ± 0.02	2.44 ± 0.54	2.82 ± 0.44	1.17 ± 0.15
29kD	mAb-9	1.97 ± 0.23	2.20 ± 0.30	1.12 ± 0.02	1.44 ± 0.34	1.90 ± 0.14	1.36 ± 0.31	1.95 ± 0.50	3.23 ± 1.62	1.57 ± 0.50
	mAb-10	13.00 ± 3.64	1352.47 ± 465.91	103.43 ± 13.97	10.45 ± 0.69	786.37 ± 51.69	75.57 ± 8.74	5.92 ± 2.85	691.17 ± 325.18	117.67 ± 6.11
	mAb-11	0.62 ± 0.25	151.97 ± 4.38	269.67 ± 92.22	0.68 ± 0.22	101.12 ± 1.53	160.67 ± 59.53	0.75 ± 0.22	112.11 ± 39.51	148.67 ± 22.74
	mAb-12	5.02 ± 1.01	2.16 ± 0.33	0.45 ± 0.16	5.48 ± 1.42	1.59 ± 0.08	0.30 ± 0.07	3.21 ± 0.73	4.83 ± 2.07	1.45 ± 0.34
48kD	mAb-13	1.41 ± 0.17	2.03 ± 0.67	1.44 ± 0.40	1.52 ± 0.23	1.14 ± 0.03	0.76 ± 0.14	1.40 ± 0.06	2.77 ± 0.29	1.99 ± 0.29
	mAb-14	7.58 ± 1.40	744.33 ± 7.37	100.43 ± 18.28	6.63 ± 1.49	598.20 ± 106.82	93.20 ± 27.30	4.91 ± 0.12	482 ± 18.12	98.03 ± 2.67
	mAb-15	3.26 ± 0.21	1.98 ± 0.60	0.61 ± 0.21	3.25 ± 0.01	1.09 ± 0.05	0.34 ± 0.02	2.36 ± 0.13	2.89 ± 0.51	1.23 ± 0.21
	mAb-16	6.16 ± 0.68	6.56 ± 0.83	1.06 ± 0.04	5.65 ± 0.14	5.34 ± 0.06	0.94 ± 0.03	2.99 ± 0.26	6.95 ± 0.76	2.33 ± 0.27
92kD	mAb-17	2.31 ± 0.83	2.73 ± 1.36	1.15 ± 0.20	1.94 ± 0.14	0.79 ± 0.05	0.41 ± 0.06	2.04 ± 0.01	1.48 ± 0.05	0.73 ± 0.02
	mAb-18	0.73 ± 0.22	2.41 ± 1.80	3.05 ± 1.38	0.61 ± 0.04	0.87 ± 0.04	1.44 ± 0.12	1.08 ± 0.39	1.48 ± 0.13	1.50 ± 0.55
	mAb-19	1.55 ± 0.76	6.11 ± 0.94	4.47 ± 1.82	1.41 ± 0.26	2.21 ± 0.13	1.62 ± 0.40	2.16 ± 0.07	2.78 ± 0.19	1.29 ± 0.10
	mAb-20	2.14 ± 0.72	3.12 ± 1.53	1.42 ± 0.26	1.90 ± 0.15	1.03 ± 0.06	0.55 ± 0.07	2.10 ± 0.02	2.08 ± 0.09	0.99 ± 0.04
105kD	mAb-21	0.51 ± 0.04	3.94 ± 0.16	7.70 ± 0.71	0.53 ± 0.09	2.78 ± 0.39	5.28 ± 0.24	0.88 ± 0.04	4.27 ± 0.47	4.89 ± 0.74
	mAb-22	1.53 ± 0.14	2.08 ± 0.24	1.36 ± 0.10	2.21 ± 0.41	2.08 ± 0.59	0.93 ± 0.10	2.04 ± 0.37	2.68 ± 0.47	1.33 ± 0.30
	mAb-23	2.89 ± 0.25	128.82 ± 29.83	44.10 ± 6.73	4.15 ± 1.50	82.76 ± 3.01	21.33 ± 5.84	3.28 ± 0.03	79.42 ± 1.19	24.23 ± 0.35
	mAb-24	2.47 ± 1.45	12.83 ± 0.85	7.46 ± 5.85	3.25 ± 1.69	13.12 ± 1.53	5.02 ± 2.90	1.68 ± 0.33	13.75 ± 0.47	8.35 ± 1.54